General, efficient, and robust Hamiltonian engineering

P. Baßler, 1, * M. Heinrich, 1, 2 and M. Kliesch 3, †

¹Heinrich Heine University Düsseldorf, Faculty of Mathematics and Natural Sciences, Düsseldorf, Germany
²Institute for Theoretical Physics, University of Cologne, Cologne, Germany[†]
³Hamburg University of Technology, Institute for Quantum Inspired and Quantum Optimization, Hamburg, Germany

Implementing the time evolution under a desired target Hamiltonian is critical for various applications in quantum science. Due to the exponential increase of parameters in the system size and due to experimental imperfections this task can be challenging in quantum many-body settings.

We introduce an efficient and robust scheme to engineer arbitrary local many-body Hamiltonians. This is achieved by applying simple single-qubit gates simultaneously to an always-on system Hamiltonian, which we assume to be native to a given platform. These sequences are constructed by efficiently solving a linear program (LP) which minimizes the total evolution time. In this way, we can engineer target Hamiltonians that are only limited by the locality of the Pauli terms in the system Hamiltonian. Based on average Hamiltonian theory and by using robust composite pulses, we make our schemes robust against errors including finite pulse time errors and various calibration errors.

To demonstrate the performance of our scheme, we provide numerical simulations. In particular, we solve the Hamiltonian engineering problem for arbitrary two-body Hamiltonians on a 2D square lattice with 225 qubits in only 60 seconds. Moreover, we simulate the time evolution of Heisenberg Hamiltonians for smaller system sizes with a fidelity larger than 99.9%, which is orders of magnitude better than non-robust implementations.

I. INTRODUCTION

Simulating a target Hamiltonian on a quantum system is a central problem in quantum computing, with applications in general gate-based and digital-analog quantum computing, as well as quantum simulations [1–6] and quantum chemistry [7–9]. It is commonly believed that simulating the dynamics of a quantum system is one of the most promising tasks for showing a practical advantage of quantum computers over classical computers [7, 10, 11], perhaps already on noisy and intermediate scale quantum (NISQ) devices [12, 13]. Especially for the latter, it is essential to have an efficient and fast implementation of the target Hamiltonian due to short coherence times.

The idea to engineer a target Hamiltonian by interleaving the evolution under a fixed system Hamiltonian with single-qubit gates originated in the nuclear magnetic resonance (NMR) community. However, the first approaches require additional single-qubit gates to decouple interactions, rescale them, and couple them again, resulting in long pulse sequences [14–18]. Recently, there has been a renewed interest in designing pulse sequences to change the effective dynamics governed by a given Hamiltonian. In particular, there has been impressive progress in the design of robust global pulses, identical pulses on each qubit, to change the global properties of a given Hamiltonian [19]. This approach has already been generalized to qudit systems [20, 21] and implemented in experiments with ultracold atomic Rydberg gas and NV centers in diamond [22, 23]. In our work, we design robust sequences of local pulses to change any interaction coupling in a given Hamiltonian, with similar robustness properties as for global pulses [19]. However, due to the local pulses in our method we are able to implement the dynamics of a much larger family of target Hamiltonians.

So far, other approaches utilizing local pulses have certain limitations. They either require NP-hard classical pre-processing to find the pulse sequence [24], rely on specific structures in the system Hamiltonian [25], or require an infinite single-qubit gate set which might be a problem for the fast control electronics in an experiment [26–28]. These works are also limited to two-body interactions, and to the best of our knowledge, no general scheme has been developed for efficiently engineering individual many-body interactions. Since there has been an increasing effort in realizing the latter in experiments [4, 29-32], such a general scheme would allow to simulate quantum chemistry Hamiltonians with genuine many-body interactions. Moreover, some recent Hamiltonian learning schemes rely on "reshaping" unknown many-body Hamiltonians to diagonal Hamiltonians which can be efficiently done with our proposed method [33-35].

In previous works, we have proposed a Hamiltonian engineering method for Ising Hamiltonians based on linear programming and applied it to multi-qubit gate synthesis and compiling problems [36, 37]. A related linear program approach for commuting Ising and next-neighbour interactions with an efficient relaxation was introduced in Refs. [38, 39].

In this work, we generalize the linear programming method to a significantly larger family of local Hamiltonians and make it substantially more efficient. More concretely, our method allows to efficiently engineer arbitrary target Hamiltonians, the interaction graph of which agrees with the one of the system Hamiltonian. To this

^{*} bassler@hhu.de

[†] martin.kliesch@tuhh.de

[‡] markus.heinrich@uni-koeln.de

end, free evolutions under the system Hamiltonian are interleaved with Pauli or single-qubit Clifford gates. A crucial feature of our method is that it minimizes the total evolution time, leading to a fast implementation of the target Hamiltonian. For larger systems, optimally solving the minimizing linear program is, however, no longer efficiently possible. To this end, we introduce a relaxation that only scales with the number of interaction terms and not directly with the system size, and thus, provides an efficient method to engineer Hamiltonians. This relaxation still yields an exact decomposition of the target Hamiltonian, but the total evolution time may no longer be minimal. The latter can, however, be decreased by expanding the search space for the relaxed problem, providing a trade-off between the runtime of the classical pre-processing and the evolution time of the implementation. For r interactions in the interaction graph of the system Hamiltonian (r free parameters), we propose an efficient method for finding the single-qubit gate sequence which only scales linear with r, i.e. not directly dependent on the number of qubits. To implement the target evolution with a product formula, we therefore only require 2Cr single-qubit gate layers, where C is a constant only depending on the chosen product formula. Note that similar previous approaches require $O(r^2)$ single-qubit gate layers [14–18] or are classically hard to solve [24]. We also observe that the total evolution time to implement the dynamics under the target Hamiltonian scales only sublinear with the number of qubits.

We also investigate the effects of dominant experimental error sources and introduce a general framework to cancel them. To this end, we generalize a method by Votto et al. [18] based on average Hamiltonian theory (AHT) to mitigate these errors. As a result, we are able to make our methods robust against finite pulse time and single-qubit rotation angle errors. We leverage the generality of our method to combine it with robust composite pulses, making it robust against many experimental error sources.

In section III we provide a general framework for engineering Hamiltonians using a linear program (LP). In sections III A and III B the efficient Hamiltonian engineering method by Pauli and Clifford conjugation are presented. In section IV we provide methods to investigate and mitigate the effect of errors on both, the Pauli and Clifford conjugation methods. Finally, in section V we show the efficiency and robustness of our methods in numerical simulations of a realistic setting.

II. PRELIMINARIES

We denote by P^n the set of *n*-qubit Pauli operators, which can be indexed by binary vectors $\boldsymbol{a}=(\boldsymbol{a}_x,\boldsymbol{a}_z)\in\mathbb{F}_2^{2n}$ such that

$$P_{\boldsymbol{a}} = P_{(\boldsymbol{a}_x, \boldsymbol{a}_z)} = i^{\boldsymbol{a}_x \cdot \boldsymbol{a}_z} X(\boldsymbol{a}_x) Z(\boldsymbol{a}_z). \tag{1}$$

Here, $X(x) := X^{x_1} \otimes \cdots \otimes X^{x_n}$ and $Z(z) := Z^{z_1} \otimes \cdots \otimes Z^{z_n}$ where X, Z are the single-qubit Pauli matrices. Sometimes, we also call P_a a Pauli string. They satisfy the following commutator relation

$$P_{\mathbf{a}}P_{\mathbf{b}} = (-1)^{\langle \mathbf{a}, \mathbf{b} \rangle} P_{\mathbf{b}} P_{\mathbf{a}} , \qquad (2)$$

for any $\boldsymbol{a}, \boldsymbol{b} \in \mathbb{F}_2^{2n}$ with the binary symplectic form on \mathbb{F}_2^{2n} defined by $\langle \boldsymbol{a}, \boldsymbol{b} \rangle \coloneqq \boldsymbol{a}_x \cdot \boldsymbol{b}_z + \boldsymbol{a}_z \cdot \boldsymbol{b}_x$, where the sum is taken in \mathbb{F}_2 , i.e., modulo 2. We refer to the identity as $I \in \mathbb{C}^{2 \times 2}$ and Pauli matrices as $X, Y, Z \in \mathbb{C}^{2 \times 2}$. The identity operator on n qubits is denoted by $\mathbb{1}_n \in \mathbb{C}^{2^n \times 2^n}$, and often we write $\mathbb{1}$ instead of $\mathbb{1}_n$.

The set P^n forms a basis for the complex matrices, i.e. any $H\in\mathbb{C}^{2^n\times 2^n}$ can be written as

$$H = \sum_{\boldsymbol{a} \in \mathbb{F}_2^{2n}} J_{\boldsymbol{a}} P_{\boldsymbol{a}} , \qquad (3)$$

with $J_{\boldsymbol{a}} \in \mathbb{C}$. If H is a Hermitian operator, which we denote by $H \in \operatorname{Herm}(\mathbb{C}^{2^n})$, then $J_{\boldsymbol{a}} \in \mathbb{R}$. We collect all $J_{\boldsymbol{a}}$ in a vector $\boldsymbol{J} \in \mathbb{R}^{4^n}$ with indices $\boldsymbol{a} \in \mathbb{F}_2^{2^n}$. We define the *support* of a Pauli string $P_{\boldsymbol{a}}$ as $\operatorname{supp}(P_{\boldsymbol{a}}) := \sup(\boldsymbol{a}) := \{i \in [n] | a_{x_i} \neq 0 \text{ or } a_{z_i} \neq 0\}$, i.e. the qubit indices on which $P_{\boldsymbol{a}}$ acts non-trivially. For any constant k, we call the Hamiltonian

$$H = \sum_{\boldsymbol{a} \in \mathbb{F}_2^{2n}} J_{\boldsymbol{a}} P_{\boldsymbol{a}} \,. \tag{4}$$

k-local if $J_a = 0$ whenever $|\operatorname{supp}(a)| > k$. If H is 2-local, its interaction graph is the graph with the sites/qubits as vertices and two vertices are connected by an edge iff H has a corresponding interaction term. For higher localities, edges are replaced by hyperedges given by the supports of the P_a , resulting in an interaction hypergraph.

III. HAMILTONIAN ENGINEERING BY LINEAR PROGRAMMING

We wish to implement the time evolution of a target Hamiltonian H_T by having access to some simple gates (e.g., certain single-qubit gates) plus the time evolution under some system Hamiltonian H_S . The system Hamiltonian can be an arbitrary Hamiltonian that is native to the considered quantum platform. That is, we wish to change H_S to achieve an effective Hamiltonian H_T . To this end, we write H_S and H_T in their Pauli decompositions

$$H_S = \sum_{\boldsymbol{a} \in \mathbb{F}_2^{2n} \setminus \{\boldsymbol{0}\}} J_{\boldsymbol{a}} P_{\boldsymbol{a}}, \qquad H_T = \sum_{\boldsymbol{a} \in \mathbb{F}_2^{2n} \setminus \{\boldsymbol{0}\}} A_{\boldsymbol{a}} P_{\boldsymbol{a}}, \quad (5)$$

with $J_{\boldsymbol{a}}, A_{\boldsymbol{a}} \in \mathbb{R}$. We exclude the term $P_{\boldsymbol{0}} = P_{(0,\dots,0)} = I^{\otimes n}$, leading to a global and thus unobservable phase. Our goal is to simulate the time evolution under H_T by the one under H_S interleaved with layers of single-qubit gates. Recall that we have the identity $\mathrm{e}^{-\mathrm{i}tU^{\dagger}HU} =$

 $U^{\dagger} e^{-itH} U$ for any Hamiltonian H and unitary U. Hence, we seek a decomposition of the form

$$H_T = \sum_{i=1}^{L} \lambda_i \mathbf{S}_i^{\dagger} H_S \mathbf{S}_i \,, \tag{6}$$

with $\lambda_i > 0$ and $S_i = S_i^{(1)} \otimes \cdots \otimes S_i^{(n)}$ representing a layer of single-qubit gates, which we later set to be either Pauli or Clifford gates. Indeed, if all terms in eq. (6) mutually commute, then the time evolution under H_T for time t can be implemented exactly by the time evolution under H_S interleaved with layers of single-qubit gates $S_i S_{i-1}^{\dagger}$ at times $t' = t \sum_{j=1}^{i-1} \lambda_j$ for $i \geq 1$ (setting $S_0 = S_{L+1} = 1$). In this way, the time evolution under Hamiltonians $S_i^{\dagger} H_S S_i$ is effectively implemented for consecutive times $t\lambda_i$ with $i = 1, 2, \ldots$ and leads to the overall time evolution under H_T . If the terms in eq. (6) do not commute, then the time evolution under H_T can be approximated in a similar fashion as for the commuting terms, utilizing suitable Hamiltonian simulation methods (e.g. product formulas).

The suitability of this approach depends highly on the decomposition (6). We base our Hamiltonian engineering method on linear programming, which allows us to both minimize the total evolution time and reduce the number of terms, i.e. layers, in Eq. (6). To this end, we consider the effect of $H_S \mapsto \mathbf{S}_i^{\dagger} H_S \mathbf{S}_i$ on the Pauli coefficients J_a which can be captured by a column vector $W_i \in \mathbb{R}^r$ with elements

$$W_{\boldsymbol{a},i} = \frac{1}{2^n} \operatorname{Tr} \left(P_{\boldsymbol{a}} \left(\boldsymbol{S}_i^{\dagger} H_S \boldsymbol{S}_i \right) \right). \tag{7}$$

Here, r is the number of Pauli terms $\{P_a\}$ we can generate from the ones in H_S by any S_i . Let s be the number of possible single-qubit layers on n qubits, and define the matrix $\mathcal{W} \in \mathbb{R}^{r \times s}$ by taking all vectors \mathcal{W}_i as columns. Then, a decomposition (6) can be found by solving the following LP minimizing the total relative evolution time:

minimize
$$\mathbf{1}^T \boldsymbol{\lambda}$$

subject to $\mathcal{W} \boldsymbol{\lambda} = \boldsymbol{A}$, $\boldsymbol{\lambda} \in \mathbb{R}^s_{>0}$, (LP)

where $\mathbf{1} = (1, 1, ..., 1)$ is the all-ones vector such that $\mathbf{1}^T \boldsymbol{\lambda} = \sum_i \lambda_i$ and $\boldsymbol{A} \in \mathbb{R}^r$ represents the Pauli coefficients of the target Hamiltonian H_T . Conjugation of H_S with arbitrary single-qubit gates yields a r which is limited by the interaction graph of H_S .

(LP) is central for our approach to Hamiltonian engineering and its analysis plays an important role in this work. For this purpose, we require some basic notions and properties from the theory of linear programming [40] which we will briefly introduce in the following. A feasible solution λ is a vector which satisfies all constraints of (LP). An optimal solution is a feasible solution that also minimizes the objective function and is indicated by an asterisk as λ^* . If (LP) has a feasible solution, then there also exists a r-sparse optimal solution

 λ^* [41], corresponding to a decomposition as in eq. (6) with only r terms. Such a r-sparse optimal solution can be found using the simplex algorithm which, in practice, has a runtime that scales polynomial in the problem size $r \times s$ [42, 43].

The first main contribution of our work is a hierarchy of relaxations of (LP) with drastically reduced size that still allows for an exact decomposition as in eq. (6). For this, we need general sufficient conditions on the matrix W such that (LP) has a feasible solution for any $A \in \mathbb{R}^r$.

Definition III.1. We say that a matrix $W \in \mathbb{R}^{r \times s}$ is feasible if for each $A \in \mathbb{R}^r$ there exists a $\lambda \in \mathbb{R}^s_{\geq 0}$ such that $W\lambda = A$.

This definition captures the constraints in (LP). There is a simple sufficient condition for the feasibility of the matrix W:

Proposition III.2. Let $W \in \mathbb{R}^{r \times s}$ such that $\ker(W^T) = \{\mathbf{0}\}$. If there exists $\mathbf{x} \in \mathbb{R}^s$ such that $W\mathbf{x} = \mathbf{0}$ and $\mathbf{x} > \mathbf{0}$, then for any $\mathbf{A} \in \mathbb{R}^r$ there exists $\mathbf{x}' \in \mathbb{R}^s$ such that $W\mathbf{x}' = \mathbf{A}$ and $\mathbf{x}' \geq \mathbf{0}$.

This proposition follows directly from two well-known results in convex analysis.

Lemma III.3 (Farkas [44]). Let $W \in \mathbb{R}^{r \times s}$ and $A \in \mathbb{R}^r$. Then exactly one of the following assertions is true:

- 1. $\exists x \in \mathbb{R}^s \text{ such that } \mathcal{W}x = A \text{ and } x > 0.$
- 2. $\exists y \in \mathbb{R}^r \text{ such that } \mathcal{W}^T y \geq 0 \text{ and } \mathbf{A}^T y < 0.$

Lemma III.4 (Stiemke [45]). Let $W \in \mathbb{R}^{r \times s}$. Then exactly one of the following assertions is true:

- 1. $\exists x \in \mathbb{R}^s \text{ such that } \mathcal{W}x = \mathbf{0} \text{ and } x > \mathbf{0}.$
- 2. $\exists y \in \mathbb{R}^r \text{ such that } \mathcal{W}^T y \geq \mathbf{0}$.

Proof of Prop. III.2. We show that the second assertion of Farkas lemma is not possible. By lemma III.4, there does not exist a y such that $\mathcal{W}^T y \geq 0$. From $\ker(\mathcal{W}^T) = \{0\}$ it follows that if $\mathcal{W}^T y = 0$, then y = 0 which contradicts $\mathbf{A}^T y < 0$ in the second assertion of lemma III.3. Finally, the case $\mathcal{W}^T y < 0$ directly contradicts the second assertion of lemma III.3.

To provide a geometric interpretation of proposition III.2 we first define the convex hull of the column vectors of \mathcal{W}

$$conv(\mathcal{W}) := \left\{ \boldsymbol{u} \in \mathbb{R}^r \,\middle|\, \mathcal{W} \boldsymbol{x} = \boldsymbol{u}, \boldsymbol{x} \ge \boldsymbol{0}, \sum_i x_i = 1 \right\},$$
(8)

and the $interior\ of\ a\ polytope\ P$

$$\inf(P) := \{ \boldsymbol{u} \in P \mid \exists \varepsilon > 0 \text{ s.t. } \|\boldsymbol{u} - \boldsymbol{x}\| < \varepsilon \ \forall \boldsymbol{x} \in \mathbb{R}^r \Rightarrow \boldsymbol{x} \in P \}.$$
(9)

(LP) is feasible if the convex hull of the column vectors of W has an interior that contains the origin, $\mathbf{0} \in$

 $\operatorname{int}(\operatorname{conv}(\mathcal{W}))$. The conditions of proposition III.2 can be efficiently verified: If the LP

minimize
$$\mathbf{1}^T \boldsymbol{x}$$

subject to $\mathcal{W} \boldsymbol{x} = \mathbf{0}$, (10)
 $\boldsymbol{x} \ge \mathbf{1}$

has a feasible solution and \mathcal{W} has full rank, then \mathcal{W} is feasible. Note that proposition III.2 applies to general matrices and will be useful for the efficient relaxations.

Numerical implementation All LPs and mixed integer linear programs (MILPs) in our work are modelled with the Python package CVXPY [46, 47] and solved with the MOSEK solver [48] on a workstation with 130 GB RAM and the AMD Ryzen Threadripper PRO 3975WX 32-Cores processor. Furthermore, we made the code to reproduce all figures in this work publicly available on GitHub [49].

A. Pauli conjugation

Conjugation of a system Hamiltonian ${\cal H}_S$ with a Pauli string $P_{\pmb b}$ leads to

$$P_{\mathbf{b}}^{\dagger} H_S P_{\mathbf{b}} = \sum_{\mathbf{a} \in \mathbb{F}_2^{2n} \setminus \{\mathbf{0}\}} (-1)^{\langle \mathbf{a}, \mathbf{b} \rangle} J_{\mathbf{a}} P_{\mathbf{a}}, \qquad (11)$$

which follows from the commutation relations (2). We seek a decomposition of H_T of the form

$$H_{T} = \sum_{\boldsymbol{a} \in \mathbb{F}_{2}^{2n} \setminus \{\mathbf{0}\}} A_{\boldsymbol{a}} P_{\boldsymbol{a}}$$

$$= \sum_{\boldsymbol{b} \in \mathbb{F}_{2}^{2n}} \lambda_{\boldsymbol{b}} P_{\boldsymbol{b}}^{\dagger} H_{S} P_{\boldsymbol{b}}$$

$$= \sum_{\boldsymbol{a} \neq \mathbf{0}, \boldsymbol{b}} \lambda_{\boldsymbol{b}} (-1)^{\langle \boldsymbol{a}, \boldsymbol{b} \rangle} J_{\boldsymbol{a}} P_{\boldsymbol{a}} , \quad (\lambda_{\boldsymbol{b}} \geq 0) .$$
(12)

The $4^n \times 4^n$ matrix with entries $W_{ab} = (-1)^{\langle a,b \rangle}$ is called the Walsh-Hadamard matrix. Here, we only need a submatrix $W^{(r \times s)} \in \{-1,1\}^{r \times s}$ defined by choosing r rowindices $a \in \mathbb{F}_2^{2n}$ and s column-indices $b \in \mathbb{F}_2^{2n}$. We call $W^{(r \times s)}$ a partial Walsh-Hadamard matrix. By eq. (12), it is clear that only the Pauli terms with $J_a \neq 0$ contribute to the target Hamiltonian H_T . Therefore, we define $\operatorname{nz}(J) \coloneqq \left\{a \in \mathbb{F}_2^{2n} \setminus \{\mathbf{0}\} \mid J_a \neq 0\right\}$, and require that the Pauli coefficients satisfy

$$nz(\boldsymbol{A}) \subseteq nz(\boldsymbol{J}).$$
 (13)

This requirement can be eliminated with single-qubit Clifford conjugation, which we will discuss in detail in section IIIB. In addition to the restriction $a \in \operatorname{nz}(J)$ given by the system Hamiltonian, we may also restrict the set of Pauli strings $b \in \mathcal{F} \subseteq \mathbb{F}_2^{2n}$, as long as there is still a solution to eq. (12). Comparing the Pauli coefficients in eq. (12), we can write this as

$$A_{\boldsymbol{a}} = J_{\boldsymbol{a}} \sum_{\boldsymbol{b} \in \mathcal{F}} W_{\boldsymbol{a}\boldsymbol{b}}^{(r \times s)} \lambda_{\boldsymbol{b}} \quad \forall \boldsymbol{a} \in \operatorname{nz}(\boldsymbol{J}),$$
 (14)

with the number of non-zero Pauli coefficients $r := |\operatorname{nz}(J)|$ and $s = |\mathcal{F}|$. Hence, the constraint in (LP) becomes $A = J \odot (W^{(r \times s)} \lambda)$, where \odot denotes elementwise multiplication and $A, J \in \mathbb{R}^r$ are restricted to $a \in \operatorname{nz}(J)$. For the following analysis, it is convenient to set $M := A \oslash J$ using the element-wise division $(A \oslash J)_a := A_a/J_a$ for all $a \in \operatorname{nz}(J)$. This results in the following LP:

minimize
$$\mathbf{1}^T \boldsymbol{\lambda}$$

subject to $W^{(r \times s)} \boldsymbol{\lambda} = \boldsymbol{M}$, $\boldsymbol{\lambda} \in \mathbb{R}^s_{\geq 0}$. (PauliLP)

The runtime of a LP scales with its size, i.e. the number of constraints r and the number of variables s. We discuss in detail the existence of a solution $\boldsymbol{\lambda} \in \mathbb{R}^{4^n}_{>0}$ and bounds on the total relative evolution time $\mathbf{1}^T \boldsymbol{\lambda}$ in appendix A. Here, $r = |nz(\boldsymbol{J})| \le 4^n - 1$ is fixed by the system Hamiltonian and a priori $s = 4^n$, thus solving (PauliLP) becomes computationally intensive already at moderate system size. To overcome this, we propose a simple and efficient relaxation of (PauliLP) in section III A 1: For any $r = |nz(\mathbf{J})|$, we sample $s \geq 2r$ Pauli strings at random, leading to a feasible LP with high probability. As we have r = poly(n) for local Hamiltonians, this indeed yields an efficient relaxation in the system size n. Note that this relaxation still leads to an exact decomposition; however, the relative evolution time $\mathbf{1}^T \boldsymbol{\lambda}$ may not be minimal anymore.

1. Efficient relaxation

We provide an efficient method to construct a feasible matrix $W^{(r \times s)}$ with $r = |\mathrm{nz}(\boldsymbol{J})|$ rows and $s \geq 2r$ columns. The construction is rather simple and consists of sampling s vectors $\boldsymbol{b} \in \mathbb{F}_2^{2n}$ uniformly at random and taking the corresponding partial Walsh-Hadamard matrix with entries $W_{\boldsymbol{ab}}^{(r \times s)} = (-1)^{\langle \boldsymbol{a}, \boldsymbol{b} \rangle}$ where $\boldsymbol{a} \in \mathrm{nz}(\boldsymbol{J})$. Thus, engineering a Hamiltonian with r non-zero Pauli terms leads to a (PauliLP), whose number of constraints and variables both scale linearly with r.

To ensure feasibility of the sub-sampled matrix, we invoke proposition III.2. Thus, we have to check that $\operatorname{conv}(W^{(r\times s)})$ has a non-empty interior and $\mathbf{0} \in \operatorname{conv}(W^{(r\times s)})$. First, we state general results for i.i.d. copies $\boldsymbol{x}_1,\ldots,\boldsymbol{x}_s$ of a random vector \boldsymbol{x} . Then, we relate the results to the partial Walsh-Hadamard matrix $W^{(r\times s)}$. Here, we assume that s is large enough and that $\boldsymbol{x}_1,\ldots,\boldsymbol{x}_s$ are in general position such that $\operatorname{conv}(\boldsymbol{x}_1,\ldots,\boldsymbol{x}_s)$ always has non-empty interior. Thus, we focus on the condition $\mathbf{0} \in \operatorname{conv}(\boldsymbol{x}_1,\ldots,\boldsymbol{x}_s)$.

Definition III.5. Let $x_1, ..., x_s$ be i.i.d. copies of an arbitrary random vector x in \mathbb{R}^r and define

$$p_{s,\boldsymbol{x}} := \mathbb{P}(\boldsymbol{0} \in \text{conv}(\boldsymbol{x}_1, \dots, \boldsymbol{x}_s)).$$
 (15)

Intuitively, one would expect that the probability should increase quickly with the number of samples s, and taking s of the order of r should make $p_{s,x}$ reasonably large.

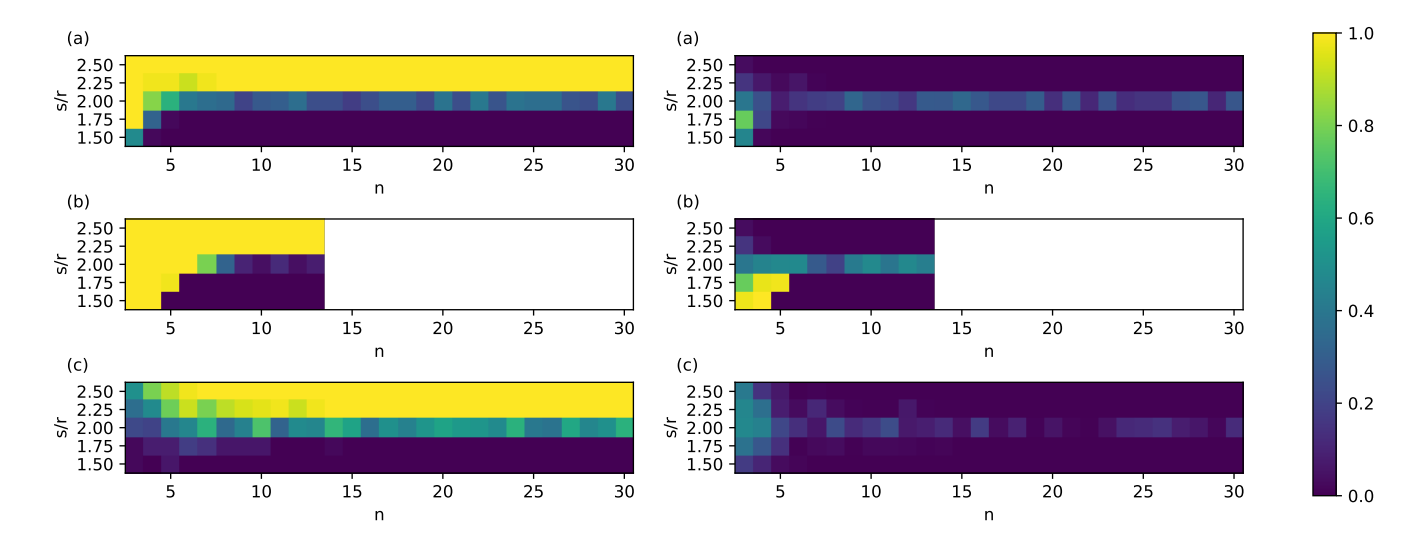


Figure 1. Select r rows of the Walsh-Hadamard matrix to obtain the partial Walsh-Hadamard matrix $W^{(r \times 4^n)}$, then randomly sample s columns to obtain $W^{(r \times s)}$. (a) and (b): For a k-local system Hamiltonian with $k \le 2$ and $k \le 3$ respectively, resulting in $r = \sum_{i=1}^k 3^i \binom{n}{i}$ Pauli terms. (b): We stopped the numerical experiments at n = 13 due to the large amount of all-to-all interactions with support $k \le 3$. (c): For random Hamiltonians with $r = n^2$ Pauli terms selected uniformly at random. Left: The plots show the success frequency for " $W^{(r \times s)}$ is feasible" over 50 samples (yellow) for $n = 3, \ldots, 30$ and $s/r = 1.5, \ldots, 2.5$. There is a sharp transition at s/r = 2 in all cases. Right: The difference of our numerical observation to Wendel's formula (17).

Lemma III.6 ([50], Proposition 4). Let $\mathbf{x} \in \mathbb{R}^r$ be an arbitrary random vector with $\mathbb{E}[\mathbf{x}] = 0$ and $\mathbb{P}(\mathbf{x} \neq 0) > 0$. Then we have

$$0 < p_{r+1,\boldsymbol{x}} < p_{r+2,\boldsymbol{x}} < \dots < p_{r+l,\boldsymbol{x}} \to 1 \quad \text{for } l \to \infty,$$

$$\text{and } p_{s,\boldsymbol{x}} = 0 \text{ if } s \le r.$$

$$(16)$$

Indeed, letting \boldsymbol{w} be the r-dimensional random vector drawn uniformly from the columns of the partial Walsh-Hadamard matrix $W^{(r\times 4^n)}$, we can readily verify $\mathbb{E}[\boldsymbol{w}]=0$ and thus lemma III.6 applies. However, the question of how large s shall be taken still remains. In the convex geometry literature, we find an elegant solution, at least for spherically symmetric random vectors, in the form of **Wendel's theorem** [51]: If the random vector \boldsymbol{x} has a spherically symmetric distribution around $\boldsymbol{0}$, then the probability (15) is given by

$$p_{s,x} = 1 - \frac{1}{2^{s-1}} \sum_{k=0}^{r-1} {s-1 \choose k}.$$
 (17)

This distribution shows a sharp transition from ≈ 0 to ≈ 1 at s = 2r. Wendel's theorem does however not apply to the random columns \boldsymbol{w} of $W^{(r \times 4^n)}$ because of the lack of spherical symmetry (see appendix B for details). Instead, the result (17) of Wendel's theorem provides an upper bound on the probabilities $p_{s,\boldsymbol{w}}$ [50, 52], and adequate lower bounds prove to be tricky to derive.

Nevertheless, we numerically observe that the random columns \boldsymbol{w} of $W^{(r \times 4^n)}$ follow the behavior that we would expect from Wendel's theorem: We observe a sharp transition of $p_{s,\boldsymbol{w}}$ at the same position as for spherical symmetric distributions, approximating the upper

bound (17). In this sense, $p_{s,\boldsymbol{w}}$ is optimal, maximizing the success probability for finding a feasible $W^{(r\times s)}$.

Numerical Observation III.7 (figure 1). Let $W^{(r \times 4^n)}$ be a partial Walsh-Hadamard matrix with $r = |\text{nz}(\boldsymbol{J})|$, and let \boldsymbol{w} be a r-dimensional random vector drawn uniformly from $\text{col}(W^{(r \times 4^n)})$. Then, we numerically observe that Wendel's statement (17) approximately holds, i.e. the random submatrix $W^{(r \times s)}$ is feasible with high probability provided we take $s \geq 2r$ samples of \boldsymbol{w} .

Let $W^{(r \times s)}$ be the partial Walsh-Hadamard matrix obtained from $W^{(r \times 4^n)}$ by randomly sampling s columns $m{b} \overset{\text{i.i.d.}}{\sim} \text{unif}(\mathbb{F}_2^{2n}) \text{ with } s \geq 2r. \text{ As } W^{(r \times s)} \text{ is feasible}$ with high probability, it can be used in (PauliLP) to engineer any target Hamiltonian with a Pauli decomposition compatible with the system Hamiltonian, i.e. with $nz(\mathbf{A}) \subseteq nz(\mathbf{J})$. One $W^{(r \times \tilde{s})}$ can be reused for different Hamiltonians with a Pauli decomposition with r terms, since the construction of $W^{(r\times s)}$ is independent of the choice of $\mathbf{a} \in \mathbb{F}_2^{2n} \setminus \{\mathbf{0}\}$. As $r = \mathsf{poly}(n)$ for local Hamiltonians, the relaxed (PauliLP) can be solved efficiently, and it provides an exact decomposition of the target Hamiltonian. The evolution time $\mathbf{1}^T \boldsymbol{\lambda}$ may however not be minimal anymore. The quality of the relaxation can be improved by increasing s, thus expanding the search space. This provides a flexible trade-off between the runtime of (PauliLP) and the optimality of λ , see figure 2. The number of interactions r in figure 2 grows quadratic for (a) and (c) and even cubic for (b) with the number of qubits n. However, $\sum \lambda = \mathbf{1}^T \lambda$ grows only linear with n.

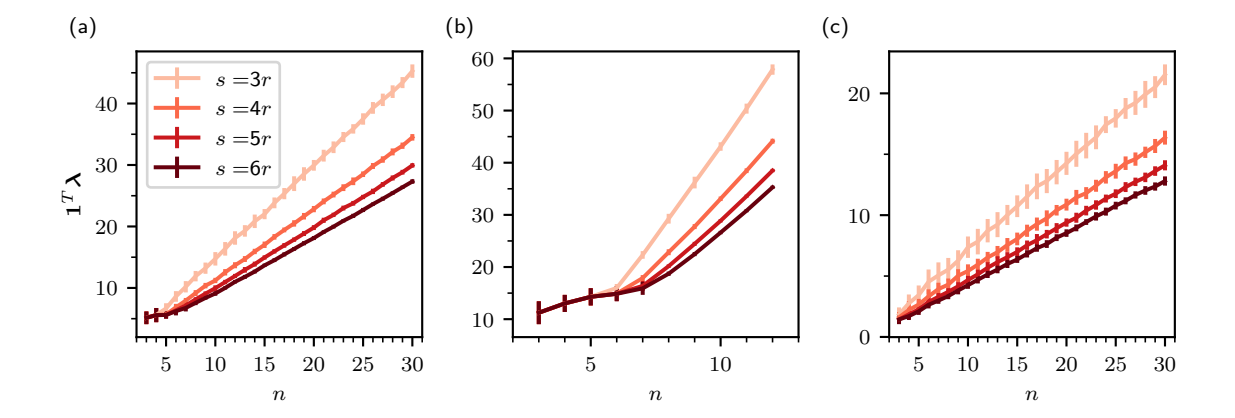


Figure 2. Solving (PauliLP) for 50 uniform random samples $M = A \oslash J$ from $[-1,1]^r$. For each sample a feasible $W^{(r \times s)}$ is generated as in numerical Observation III.7 with $s = 3r, \ldots, 6r$. The average objective function value $\sum \lambda = \mathbf{1}^T \lambda$ over the number of qubits n is shown. The error bars represent the sample standard deviation. The r interactions of the plots (a), (b) and (c) are chosen the same way as in figure 1.

B. Clifford conjugation

In section III A, we introduced the Hamiltonian engineering method based on conjugation with Pauli gates. In this section, we extend this method to a certain set of single-qubit Clifford gates. This extension allows us to change the Pauli terms in the system Hamiltonian, such the only restriction in engineering a target Hamiltonian comes from the interaction (hyper)graph of the system Hamiltonian H_S . The same restriction also holds for conjugation with arbitrary single-qubit gates, making Clifford conjugation a powerful Hamiltonian engineering method. The simplest set of single-qubit Clifford gates with full expressivity are the square-root Pauli gates ($\frac{\pi}{2}$ rotations)

$$\sqrt{X} = \frac{1}{2} \begin{pmatrix} 1+i & 1-i \\ 1-i & 1+i \end{pmatrix}, \quad \sqrt{Y} = \frac{1}{2} \begin{pmatrix} 1+i & -1-i \\ 1+i & 1+i \end{pmatrix},$$

$$\sqrt{Z} = \begin{pmatrix} 1 & 0 \\ 0 & i \end{pmatrix}.$$
(18)

$S^{\dagger}PS$	\sqrt{X}	\sqrt{Y}	\sqrt{Z}	\sqrt{X}^{\dagger}	\sqrt{Y}^{\dagger}	\sqrt{Z}^{\dagger}
X	X	Z	-Y	X	-Z	Y
Y	-Z	Y	X	Z	Y	-X
Z	Y	-X	Z	-Y	X	Z

Table I. Conjugation of Pauli gates $P \in \mathsf{P}$ with square-root Pauli gates $S \in \{\sqrt{X}, \sqrt{Y}, \sqrt{Z}, \sqrt{X}^\dagger, \sqrt{Y}^\dagger, \sqrt{Z}^\dagger\}$.

As displayed in table I, the conjugation of a Pauli gate with a square-root Pauli gate does not only flip the sign but also changes the interaction type (rotation axis). The change of the interaction type increases the set of Hamiltonians reachable by Clifford conjugation compared to the Pauli conjugation. In the following, we consider a gate set that behaves very similar to the

conjugation with Pauli gates:

$$\mathcal{C}_{XY} := \{Z\} \cup \left\{ QD \mid Q, D \in \{\sqrt{X}, \sqrt{Y}, \sqrt{X}^{\dagger}, \sqrt{Y}^{\dagger}\} \right\}.$$

Likewise, we can define gate sets \mathcal{C}_{ZY} and \mathcal{C}_{XZ} , for which conclusions analogous to the following ones may be drawn. Conjugation of Pauli terms with the Clifford gates $\sqrt{X}\sqrt{Y}$ or $\sqrt{Y}^\dagger\sqrt{X}^\dagger$ changes the interaction type and leaves the sign of the Pauli coefficient unchanged. The signs of the conjugated Pauli terms depend on the rotation direction, i.e. the placement of "†", of the squareroot Pauli gates; see table II for examples. Therefore, we label an element in \mathcal{C}_{XY} by $c \coloneqq (p, \mathbf{b}) \in \mathbb{F}_3 \times \mathbb{F}_2^2$, where $p \in \mathbb{F}_3$ represents the changes in the interaction type and $\mathbf{b} \in \mathbb{F}_2^2$ captures the sign flips similar to the Pauli conjugation. Denote $\mathcal{C}_{XY}^{\otimes n}$ a string of single-qubit gates on n qubits from the gate set \mathcal{C}_{XY} . We label each $S_c \in \mathcal{C}_{XY}^{\otimes n}$ with $\mathbf{c} = (c_1, \ldots, c_n) = (\mathbf{p}, \mathbf{b}) \in \mathbb{F}_3^n \times \mathbb{F}_2^{2n}$, where $c_i \in \mathbb{F}_3 \times \mathbb{F}_2^2$ represents the single-qubit Clifford gate from \mathcal{C}_{XY} on the i-th qubit. In table II, we show the effect of conjugating a Pauli gate $P_a \in \mathbb{P}$ with $S_c \in \mathcal{C}_{XY}$. Conjugation of H_S with $S_c \in \mathcal{C}_{XY}^{\otimes n}$ leads to

$$S_{\mathbf{c}}^{\dagger} H_{S} S_{\mathbf{c}} = \sum_{\mathbf{a} \in \mathbb{F}_{2}^{2n} \setminus \{\mathbf{0}\}} J_{\mathbf{a}} S_{\mathbf{c}}^{\dagger} P_{\mathbf{a}} S_{\mathbf{c}}$$

$$= \sum_{\mathbf{a} \in \mathbb{F}_{2}^{2n} \setminus \{\mathbf{0}\}} (-1)^{\langle \mathbf{a}, \mathbf{b} \rangle} J_{\pi_{\mathbf{p}}(\mathbf{a})} P_{\mathbf{a}},$$
(20)

with $\boldsymbol{c}=(\boldsymbol{p},\boldsymbol{b})\in\mathbb{F}_3^n\times\mathbb{F}_2^{2n}$ and the permutation $\pi_{\boldsymbol{p}}:\mathbb{F}_2^{2n}\to\mathbb{F}_2^{2n}$ with $\pi_{\boldsymbol{p}}(\boldsymbol{a}):=(\pi_{p_1}(a_1),\ldots,\pi_{p_n}(a_n))$ given by the local permutations $\pi_0,\pi_1,\pi_2:\mathbb{F}_2^2\to\mathbb{F}_2^2$ in the

c	a	(a_x, a_z)	(0,0)	(1,0)	(1, 1)	(0, 1)
p	\boldsymbol{b}	S_c P_a	I	X	Y	Z
0	(0,0)	I	I	X	Y	Z
	(1,0)	X	I	X	-Y	-Z
	(1, 1)	Y	I	-X	Y	-Z
	(0,1)	Z	I	-X	-Y	Z
1	(0,0)	$\sqrt{X}\sqrt{Y}$	I	Z	X	Y
	(1,0)	$\sqrt{X}^{\dagger}\sqrt{Y}$	I	Z	-X	-Y
	(1, 1)	$\sqrt{X}^{\dagger}\sqrt{Y}^{\dagger}$	I	-Z	X	-Y
	(0, 1)	$\sqrt{X}\sqrt{Y}^{\dagger}$	I	-Z	-X	Y
2	(0,0)	$\sqrt{Y}^{\dagger}\sqrt{X}^{\dagger}$	I	Y	Z	X
	(1,0)	$\sqrt{Y}\sqrt{X}$	I	Y	-Z	-X
	(1,1)	$\sqrt{Y}\sqrt{X}^{\dagger}$	I	-Y	Z	-X
	(0,1)	$\sqrt{Y}^{\dagger}\sqrt{X}$	I	-Y	-Z	X

Table II. The coloured cells show the conjugated Pauli gates $S_c^{\dagger} P_{\boldsymbol{a}} S_c$ for $P_{\boldsymbol{a}} \in P$ conjugated by the single-qubit Clifford gate $S_c \in \mathcal{C}_{XY}$. We label an element in \mathcal{C}_{XY} by $c \coloneqq (p, \boldsymbol{b}) \in \mathbb{F}_3 \times \mathbb{F}_2^2$, where $p \in \mathbb{F}_3$ captures the permutation of the conjugated Pauli terms, and \boldsymbol{b} captures the sign flips similar to the Pauli conjugation. This can be easily verified with table I.

two-line notation

$$\pi_0 := \begin{pmatrix} (0,0) & (1,0) & (1,1) & (0,1) \\ (0,0) & (1,0) & (1,1) & (0,1) \end{pmatrix},
\pi_1 := \begin{pmatrix} (0,0) & (1,0) & (1,1) & (0,1) \\ (0,0) & (1,1) & (0,1) & (1,0) \end{pmatrix},
\pi_2 := \begin{pmatrix} (0,0) & (1,0) & (1,1) & (0,1) \\ (0,0) & (0,1) & (1,0) & (1,1) \end{pmatrix}.$$
(21)

We want to find a decomposition of H_T with $\lambda_c \geq 0$ such that

$$H_T = \sum_{\boldsymbol{a} \in \mathbb{F}_2^{2n} \setminus \{\boldsymbol{0}\}} A_{\boldsymbol{a}} P_{\boldsymbol{a}} = \sum_{\boldsymbol{c} \in \mathbb{F}_3^n \times \mathbb{F}_2^{2n}} \lambda_{\boldsymbol{c}} S_{\boldsymbol{c}}^{\dagger} H_S S_{\boldsymbol{c}}.$$
 (22)

We define the matrix $W(\boldsymbol{J}) \in \mathbb{R}^{(4^n-1)\times 12^n}$ with entries

$$W(\boldsymbol{J})_{\boldsymbol{a}\boldsymbol{c}} := (-1)^{\langle \pi_{\boldsymbol{p}}(\boldsymbol{a}), \boldsymbol{b} \rangle} J_{\pi_{\boldsymbol{p}}(\boldsymbol{a})},$$
 (23)

for $\boldsymbol{a} \in \mathbb{F}_2^{2n} \setminus \{\boldsymbol{0}\}$, excluding the identity term $P_{\boldsymbol{a}} = I^{\otimes n}$ with $\boldsymbol{a} = \boldsymbol{0}$, and $\boldsymbol{c} \in \mathbb{F}_3^n \times \mathbb{F}_2^{2n}$. Similar to the Pauli conjugation we define the submatrix $W(\boldsymbol{J})^{(r \times s)} \in \mathbb{R}^{r \times s}$ with entries given in eq. (23) for r row-indices $\boldsymbol{a} \in \mathbb{F}_2^{2n} \setminus \{\boldsymbol{0}\}$ and s column-indices $\boldsymbol{c} \in \mathbb{F}_3^n \times \mathbb{F}_2^{2n}$. Up to the permutation of \boldsymbol{J} , the same Walsh-Hadamard matrix structure as in $W^{(r \times s)}$ from section III A is present in $W(\boldsymbol{J})^{(r \times s)}$. In terms of the matrix $W(\boldsymbol{J})$ it follows that

$$H_T = \sum_{\boldsymbol{a} \in \mathbb{F}_2^{2n} \setminus \{\boldsymbol{0}\}} \sum_{\boldsymbol{c} \in \mathbb{F}_3^n \times \mathbb{F}_2^{2n}} \lambda_{\boldsymbol{c}} W(\boldsymbol{J})_{\boldsymbol{a}\boldsymbol{c}} P_{\boldsymbol{a}}.$$
 (24)

Due to the permutation in eq. (23) we are no longer restricted by the non-zero coefficients as in the Pauli conjugation. From eq. (24) it follows that for each $A_{a} \neq 0$ there has to be at least one $J_{\hat{a}} \neq 0$ such that $\operatorname{supp}(\hat{a}) = \operatorname{supp}(a)$. Therefore, we define

$$\operatorname{suppnz}(\boldsymbol{J}) \coloneqq \left\{ \boldsymbol{a} \in \mathbb{F}_2^{2n} \setminus \{\boldsymbol{0}\} \middle| \exists \hat{\boldsymbol{a}} \in \operatorname{nz}(\boldsymbol{J}), \\ \operatorname{supp}(\hat{\boldsymbol{a}}) = \operatorname{supp}(\boldsymbol{a}) \right\},$$

$$(25)$$

and require that the Pauli coefficients satisfy

$$nz(\mathbf{A}) \subseteq suppnz(\mathbf{J}).$$
 (26)

In physical terms, this means that we are only restricted by the interaction graph of the system Hamiltonian H_S and have full flexibility in the kind of interactions and the interaction strength. In addition to the restriction $a \in \text{suppnz}(J)$, given by the system Hamiltonian, we can also consider a restricted set of conjugating Clifford strings $c \in \mathcal{F} \subseteq \mathbb{F}_3^n \times \mathbb{F}_2^{2n}$, as long as there still exists a solution. Then, the restricted eq. (24) can be reformulated as

$$A_{\boldsymbol{a}} = \sum_{\boldsymbol{c} \in \mathcal{F}} W(\boldsymbol{J})_{\boldsymbol{a}\boldsymbol{c}}^{(r \times s)} \lambda_{\boldsymbol{c}} \quad \forall \boldsymbol{a} \in \operatorname{suppnz}(\boldsymbol{J}), \qquad (27)$$

with $r \coloneqq |\mathrm{suppnz}(\boldsymbol{J})|$ and $s = |\mathcal{F}|$. The constraint in (LP) then reads $\boldsymbol{A} = W(\boldsymbol{J})^{(r \times s)} \boldsymbol{\lambda}$, with $\boldsymbol{A}, \boldsymbol{J} \in \mathbb{R}^r$ restricted to $\boldsymbol{a} \in \mathrm{suppnz}(\boldsymbol{J})$. With that, we define the following LP

minimize
$$\mathbf{1}^T \boldsymbol{\lambda}$$

subject to $W(\boldsymbol{J})^{(r \times s)} \boldsymbol{\lambda} = \boldsymbol{A}, \ \boldsymbol{\lambda} \in \mathbb{R}^s_{\geq 0}$. (CliffLP)

There always exists a feasible solution of (CliffLP) with $W(\boldsymbol{J})^{(r\times 12^n)}$, which follows similarly to corollary A.1 from the Walsh-Hadamard structure in $W(\boldsymbol{J})^{(r\times 12^n)}$. In general, we have $s \leq 12^n$ and $r \leq 4^n - 1$. In the next section, we propose a simple and efficient relaxation of (CliffLP), where $s \geq 2r$ can be chosen for arbitrary $r = |\text{suppnz}(\boldsymbol{J})|$.

1. Efficient relaxation

The size of (CliffLP) scales as $O(12^n)$ if all possible Clifford layers are considered. Therefore, a relaxation is necessary to solve this LP in practice. Analogous to the Pauli conjugation method, section III A 1, sampling $s \geq 2r$ columns at random from $W(\boldsymbol{J})^{(r \times 12^n)}$ results in a feasible matrix $W(\boldsymbol{J})^{(r \times s)}$ with high probability. As in section III A 1, we test this statement numerically by checking the feasibility conditions of proposition III.2 for random submatrices.

Numerical Observation III.8 (figure 3). Let $W(\boldsymbol{J})^{(r \times 12^n)}$ be a matrix with $r = |\mathrm{suppnz}(\boldsymbol{J})|$ and entries as in eq. (23), and let \boldsymbol{w} be a r-dimensional random vector drawn uniformly from $\mathrm{col}(W(\boldsymbol{J})^{(r \times 12^n)})$. Then, we numerically observe that Wendel's statement (17) approximately holds, i.e. the random submatrix $W(\boldsymbol{J})^{(r \times s)}$ is feasible with high probability provided we take $s \geq 2r$ samples of \boldsymbol{w} .

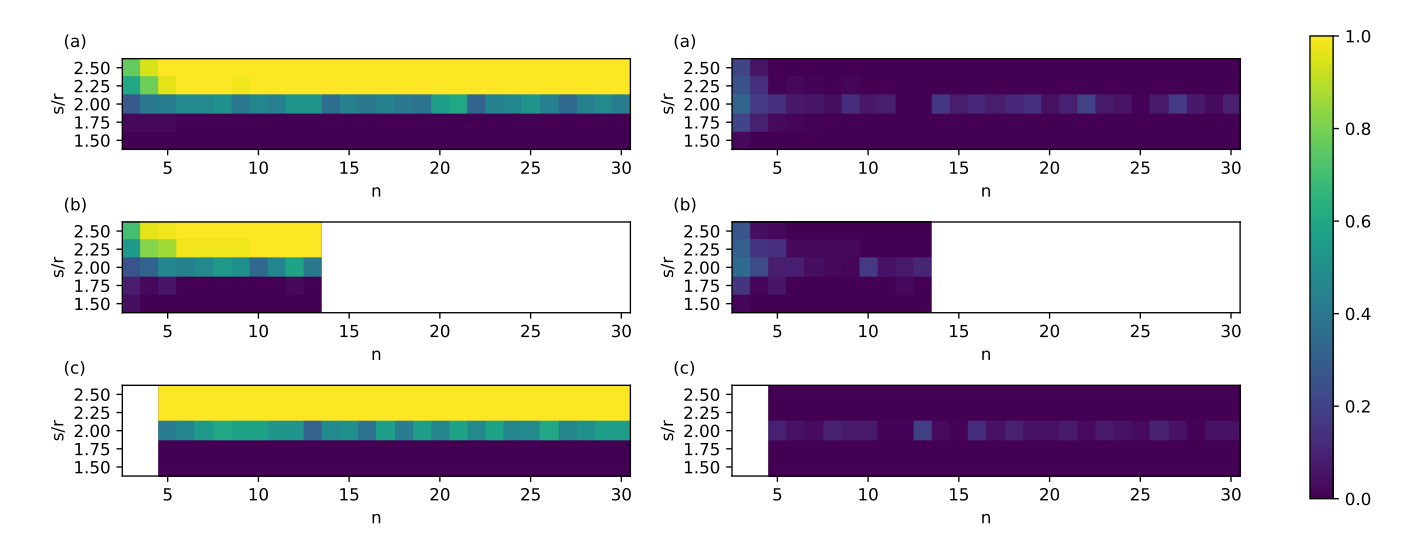


Figure 3. Select r rows of W(J) to get the partial martrix $W(J)^{(r\times 12^n)}$, then randomly sample s columns to obtain $W(J)^{(r\times s)}$. (a) and (b): For a k-local system Hamiltonian with $k \leq 2$ and $k \leq 3$ respectively, resulting in $r = \sum_{i=1}^k 3^i \binom{n}{i}$ Pauli terms. (b): We stopped the numerical experiments at n=13 due to the large amount of all-to-all interactions with support $k \leq 3$. (c): For each $k=1,\ldots,5$ choose randomly 10 different supports $\sup(a)$ and consider all possible interactions on these supports. This results in $r \leq 10 \sum_{k=1}^5 3^k$ (" \leq ", since for k=1 there are only n different supports). This represents a sparse random 5-local Hamiltonian. (a), (b), (c): For a k-local interaction term P_a there exist 3^k distinct Pauli terms $P_{a'}$ with the same support $\sup(a) = \sup(a')$, i.e. corresponding to the same (hyper)edge in the interaction graph. For each (hyper)edge the set of non-zero interactions is sampled randomly both in the interaction strength $J_a \stackrel{\text{i.i.d.}}{\sim} \min([-1,+1])$ and the interaction type (index a is chosen randomly). So, the amount, index, and values of the non-zeros in J are random. Left: The plots show the success frequency over 50 samples for " $W(J)^{(r\times s)}$ is feasible" (yellow) for each $n=3,\ldots,30$ and $s/r=1.5,\ldots,2.5$. There is a sharp transition at s/r=2 in all cases. Right: The difference of our numerical observation from Wendel's statement (17).

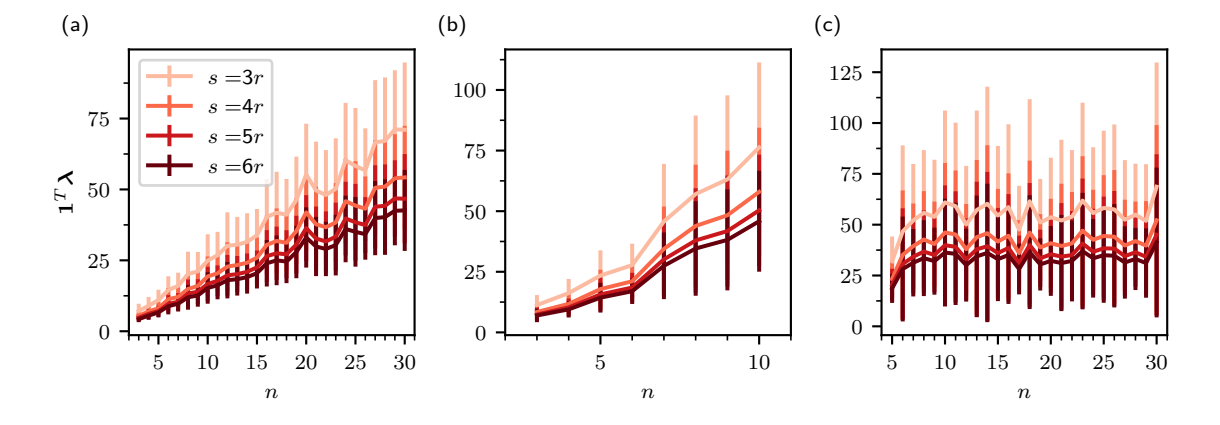


Figure 4. Solving (CliffLP) for 50 uniform random samples \boldsymbol{A} from $[-1,1]^r$. For each sample a feasible $W(\boldsymbol{J})^{(r\times s)}$ is generated as in numerical Observation III.8 with $s=3r,\ldots,6r$. The average objective function value $\sum \boldsymbol{\lambda}=\mathbf{1}^T\boldsymbol{\lambda}$ over the number of qubits n is shown. The error bars represent the sample standard deviation. The r interactions and \boldsymbol{J} of the plots (\mathbf{a}) , (\mathbf{b}) and (\mathbf{c}) are chosen the same way as in figure 3.

From the definition of feasibility, we know that (CliffLP) always has a solution for arbitrary A, i.e. arbitrary J, A such that $\operatorname{nz}(A) \subseteq \operatorname{suppnz}(J)$. Furthermore, the quality of the relaxation can be improved by increasing s, which leads to an expanded search space, see figure 4. This provides again a flexible trade-off between the runtime of (CliffLP) and the optimality of λ . The scaling of $\mathbf{1}^T\lambda$ in figure 4 (c) is independent of

n since $r \leq 10 \sum_{k=1}^5 3^k$ is independent of n. For the Clifford conjugation, the sample standard deviation is larger compared to the Pauli conjugation. This is due to the increased set of target Hamiltonians which are reachable by the Clifford conjugation. Here, we also randomly sample the number and the position of the non-zero values in J.

C. Hamiltonian engineering with unknown Hamiltonians

In practice, sometimes not all coupling coefficients in J might be known. For example, when an experiment aims to realize two-body interactions but also acquires unwanted three-body terms of unknown strength. Such system Hamiltonians with unknown or only partially known coupling strengths can still be used for engineering based on the Pauli conjugation method from section III A. Solving (PauliLP) for an $M \in \mathbb{R}^r$ yields the target Hamiltonian

$$\sum_{\mathbf{a} \in \mathbb{F}_2^{2n} \setminus \{\mathbf{0}\}} M_{\mathbf{a}} J_{\mathbf{a}} P_{\mathbf{a}} = H_T.$$
 (28)

The potentially unknown coefficients J_a are modified by an element-wise multiplication $M \odot J$. Interesting choices for M_a are -1 and 0, inverting the sign of or canceling the term P_a , respectively, without the knowledge of J_a . For each term in the system Hamiltonian, a different M_a can be chosen. Therefore, engineering known terms $M_a = A_a/J_a$ in the Hamiltonian while canceling or inverting other (potentially unknown) terms $M_a = 0$ or $M_a = -1$ is possible. Using such a M in (PauliLP) with dummy values for the unknown J_a inverts the signs or cancels the interactions.

In section VA we apply the approach to cancel unknown 3-body terms in a 2D lattice Hamiltonian.

D. Hamiltonian engineering with 2D lattice Hamiltonian

The scaling of our method is independent of the system size and only depends on the number of interactions. To highlight this fact, we consider a system Hamiltonian with a 2D square lattice interaction graph. Our Hamiltonian with constant couplings between neighboring qubits is motivated by experimental quantum platforms such as interacting superconducting qubits or cold atoms in optical lattices [53–55].

We consider a system and target Hamiltonian

$$H_S = J \sum_{i,j \in E} P_{a_i} P_{a_j} , \quad H_T = \sum_{i,j \in E} A_{a} P_{a_i} P_{a_j} , \quad (29)$$

with $\operatorname{supp}(\boldsymbol{a}) \in E$, representing all possible two-body interactions on a 2D square lattice interaction graph with the set of edges E, and constant interaction strength in the system Hamiltonian.

Figure 5 shows that a target Hamiltonian H_T with arbitrary couplings A with this interaction graph can be engineered for 225 qubits in about 60 seconds of classical runtime using the Pauli conjugation method (PauliLP).

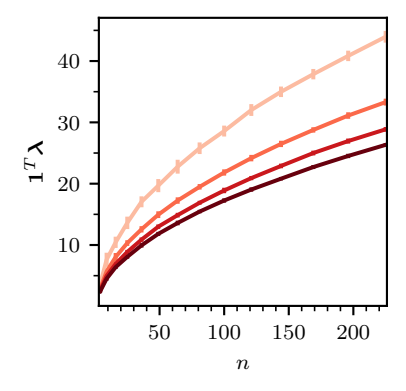
IV. ERROR ROBUSTNESS AND MITIGATION TECHNIQUES

To successfully apply the Pauli or Clifford conjugation in practice it is necessary to make the resulting pulse sequences robust against dominant errors. In this section, we provide mitigation techniques for our efficient conjugation methods, which come with little overhead. The simultaneous action of the single-qubit pulse and system Hamiltonian is called the finite pulse time error. It has been shown that this error is detrimental to approaches similar to ours [56]. Therefore, our focus lies on the error due to a finite single-qubit pulse duration. Furthermore, we provide a modification to combine our Clifford method with robust composite pulses, making it robust against many different errors occurring in experiments. We achieve robustness against finite pulse time effects and rotation angle errors using a similar approach as in Votto et al. [18]. Their study focuses on specifically designed π -pulse sequences (i.e. Pauli gates), so-called Walsh sequences, for engineering XY-Hamiltonians. In our work, we generalize their approach to general local system Hamiltonians and arbitrary single-qubit pulses.

AHT is a well-known approach in NMR that allows to investigate the dynamics under a time-dependent Hamiltonian by approximating it with the one of a time-dependent Hamiltonian [57, 58]. This approximation is done by a low order Magnus expansion [59]. We utilize AHT to investigate the error due to a finite single-qubit pulse time. We will heavily use that the error term in the average Hamiltonian has the same interaction graph as the system Hamiltonian.

In the following, we give an explicit form of the finite pulse time error in the average Hamiltonian when interleaving a system Hamiltonian with arbitrarily many layers of single-qubit pulses. For the Clifford conjugation method, we find that the finite pulse time error can be exactly cancelled by a slight modification of (CliffLP). This general investigation enables us to also mitigate finite pulse time error in combination with other pulse errors by replacing the single-qubit Clifford pulses in our Clifford conjugation method with robust composite pulses. The latter are designed to compensate for experimental errors by implementing a gate with a specific pulse sequence. In this way, dominant error sources can be cancelled or suppressed, which includes rotation angle error (Rabi frequency errors), off-resonance errors [60, 61], phase errors [62], pulse shape errors [63–65], or non-stationary, non-Markovian noise [66] or crosstalk [67].

For the Pauli conjugation method, the finite pulse time error on the interaction graph of the system Hamiltonian can only be partially mitigated by modifying (PauliLP). However, the freedom in choosing the rotation direction in the π pulse can be leveraged in addition to the modified (PauliLP) to completely cancel the finite pulse time error term in the average Hamiltonian. Moreover, this simultaneously cancels first order effects of rotation angle errors in the single-qubit pulses.



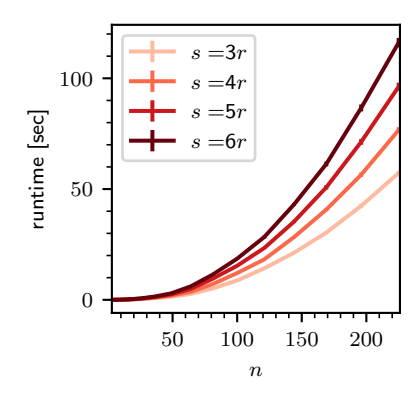


Figure 5. A two-body system Hamiltonian on a 2D square lattice with $n=4,\ldots,225$ qubits as in eq. (29) and a constant J=1. The number of interactions is $r=3^2|E|$ with the set of edges E of a 2D square lattice. We sample 50 target Hamiltonians with uniform random samples A from $[-1,1]^T$. For each sample, a feasible $W^{(r\times s)}$ is generated with $s=3r,\ldots,6r$, using the efficient method from section III A 1. Left: The average and the sample standard deviation of the objective function value $\sum \lambda = \mathbf{1}^T \lambda$ over the number of qubits n is shown. Right: The average and the sample standard deviation of the runtime for solving (PauliLP) over the number of qubits n is shown.

We introduce basic concepts required for the following chapters in section IV A. Then, in section IV B, we start with the investigation of the finite pulse time error when conjugating a system Hamiltonian with arbitrary many general single-qubit pulses. In section IV C, we apply the general results to present our robust Clifford conjugation methods. Finally, in section IV D, we present our robust Pauli conjugation method.

A. Preliminaries

For our robust methods, we require two well-known approaches to approximate the time evolution under non-commuting Hamiltonians. First, we present general Trotter product formulae to approximate the time evolution under a linear combination of time-independent Hamiltonians. Recently, the performance of the Suzuki-Trotter approximation has been greatly improved [68]. Second, we present the Magnus expansion to approximate the time evolution under a time-dependent Hamiltonian by a time-independent Hamiltonian.

1. Product formula

The time evolution under a Hamiltonian $H = \sum_{i=1}^{L} H_i$ can generally be approximated by a product formula

$$e^{-itH} \approx e^{-i\alpha_q H_{i_q}} \dots e^{-i\alpha_1 H_{i_1}},$$
 (30)

with the number of evolution steps q and $i_1, \ldots, i_q \in [L]$. We call a product formula deterministic if i_1, \ldots, i_q can be found by a deterministic algorithm. For our methods we do not require, that $\alpha_1, \ldots, \alpha_q \in \mathbb{R}$ are chosen deterministically. The best known deterministic product formulae are the Suzuki-Trotter formulae [69, 70]. The

first- and second order approximations are given by

$$e^{-itH} \approx \left(\prod_{i=1}^{L} e^{-i\frac{t}{n_{\text{Tro}}}H_i} \right)^{n_{\text{Tro}}} =: S_1(t/n_{\text{Tro}})^{n_{\text{Tro}}}$$
 (31)

and

$$e^{-itH} \approx \left(\prod_{i=1}^{L} e^{-i\frac{t}{2n_{\text{Tro}}} H_i} \prod_{i=1}^{L} e^{-i\frac{t}{2n_{\text{Tro}}} H_i} \right)^{n_{\text{Tro}}}$$

$$=: S_2(t/n_{\text{Tro}})^{n_{\text{Tro}}},$$
(32)

respectively, with the number of Trotter cycles n_{Tro} . The number of Trotter cycles can be increased to improve the accuracy. Throughout our work we use the convention $\overrightarrow{\prod}_{i=1}^L A_i := A_L \dots A_1$ and $\overleftarrow{\prod}_{i=1}^L A_i := A_1 \dots A_L$ to indicate the order of the products of non-commuting operators. The 2k-th order Suzuki-Trotter formula for k > 1 is defined recursively by

$$S_{2k}(t) := S_{2k-2}(u_k t)^2 S_{2k-2}((1-4u_k)t) S_{2k-2}(u_k t)^2,$$
(33)

with $u_k := (4 - 4^{(2k-1)^{-1}})^{-1}$. For a 2k-th order Suzuki-Trotter formula the approximation error in spectral norm is bounded by

$$||S_{2k}(t/n_{\text{Tro}})^{n_{\text{Tro}}} - e^{-itH}|| \le O\left(\left(t\sum_{i=1}^{L} ||H_i||\right)^{2k+1} n_{\text{Tro}}^{-2k}\right),$$
(34)

with the spectral norm $||H_i||$ [71].

2. Average Hamiltonian theory and the Magnus expansion

Given a time-dependent Hamiltonian H(t), it is sometimes useful to consider a time-independent effective or

average Hamiltonian $H_{\rm av}$ satisfying

$$\mathcal{U}(T) \approx e^{-iTH_{av}},$$
 (35)

where $\mathcal{U}(T)$ is the time evolution operator defined by the differential equation

$$\frac{d\mathcal{U}(t)}{dt} = -iH(t)\mathcal{U}(t), \quad \text{and} \quad \mathcal{U}(0) = \mathbb{1}.$$
 (36)

This average Hamiltonian can be expressed by the Magnus expansion as follows

$$H_{\rm AV} = H_{\rm av}^{(1)} + H_{\rm av}^{(2)} + \dots,$$
 (37)

where the first and second order terms are explicitly given by

$$H_{\text{av}}^{(1)} := \frac{1}{T} \int_0^T H(\tau) d\tau \tag{38}$$

and

$$H_{\text{av}}^{(2)} := \frac{1}{2iT} \int_0^T \int_0^\tau [H(\tau), H(\tau')] d\tau' d\tau.$$
 (39)

The Magnus expansion converges if $\int_0^T \|H(\tau)\|_2 d\tau < \pi$ [72]. As a rule of thumb, the Magnus expansion converges rapidly if

$$\max_{\tau \in [0,T]} ||H(\tau)||_2 T \ll 1, \qquad (40)$$

where the Schatten 2-norm is used [73]. Throughout this work we only consider the first order approximation and write $H_{\rm av} = H_{\rm av}^{(1)}$.

B. General robust conjugation method

We start with a general discussion of the finite pulse time error when conjugating a system Hamiltonian H_S with multiple layers of general single-qubit pulses. To this end, we define the Hamiltonian of a general single-qubit pulse layer and the operators relevant for the following discussion.

Definition IV.1. Let $\mathcal{G} \subset \operatorname{Herm}(\mathbb{C}^2)$ be a set of single-qubit pulse generators. A single-qubit pulse layer is

given by a local generator h_i chosen from \mathcal{G} for each qubit $i \in [n]$, the (single-qubit) rotation directions $\mathbf{s} \in \mathbb{F}_2^n$ and the finite pulse time $t_p > 0$. The Hamiltonian generating the single-qubit pulse layer on n qubits is given by

$$H(t_p, \boldsymbol{s}, \boldsymbol{h}) := \frac{1}{t_p} \sum_{i=1}^n (-1)^{s_i} h_i, \qquad (41)$$

with $\mathbf{h} := (h_1, \dots, h_n)$. The single-qubit pulse layer Hamiltonian is completely specified by the tuple $c := (t_p, \mathbf{s}, \mathbf{h})$, and we write $H_c := H(t_p, \mathbf{s}, \mathbf{h})$. This generates the evolution operator for one single-qubit pulse layer

 $S_c(t) := e^{-itH_c}$, and $S_c := S_c(t_p)$. (42) More generally, we consider a sequence of n_L single-qubit pulse layers and introduce the layer index $\ell \in [n_L]$. The evolution for the ℓ -th single-qubit pulse layer is specified by the tuple $c^{(\ell)} := (t_p^{(\ell)}, \mathbf{s}^{(\ell)}, \mathbf{h}^{(\ell)})$, and we define the tuple $\mathbf{c} := (c^{(1)}, \dots, c^{(n_L)})$. Moreover, we define the singlequbit pulse block and the partial single-qubit pulse block as

$$\boldsymbol{S_c} \coloneqq \prod_{\ell=1}^{n_L} \boldsymbol{S}_{c^{(\ell)}}, \qquad (43)$$

and

$$\boldsymbol{S}_{\boldsymbol{c}^{\geq D}} := \begin{cases} \overrightarrow{\prod}_{\ell=D}^{n_L} \boldsymbol{S}_{c^{(\ell)}}, & 1 \leq D \leq n_L \\ \mathbb{1}, & otherwise, \end{cases}$$
(44)

respectively. Similarly, we define the pulse time for the single-qubit pulse block $T_p \coloneqq \sum_{\ell=1}^{n_L} t_p^{(\ell)}$ and for the partial single-qubit pulse block $T_p^{\leq D} \coloneqq \sum_{\ell=1}^{D} t_p^{(\ell)}$.

To illustrate definition IV.1 we provide the Hamiltonian for the single-qubit Pauli pulses from section III A. The Hamiltonian for a single-qubit Pauli pulse layer is given by the π pulse time t_p , an arbitrary rotation direction $s \in \mathbb{F}_2^n$ and the generators $h_i = \frac{\pi}{2}P_i$, with the Pauli operator P_i given by P_{b_i} from eq. (11).

Recall from section III that ideally, we would like to implement the conjugation $S_c^{\dagger} e^{-it\lambda_c H_S} S_c = e^{-it\lambda_c S_c^{\dagger} H_S S_c}$, with the system Hamiltonian H_S and the relative evolution time λ_c associated with a single-qubit pulse block S_c . However, due to the finite duration of the single-qubit pulse we get the time evolution

$$U(t\lambda_{\mathbf{c}}) = \left(\prod_{\ell=1}^{n_L} e^{-it_p^{(\ell)}(H_S - H_{c(\ell)})}\right) e^{-it\lambda_{\mathbf{c}}H_S} \left(\prod_{\ell=1}^{n_L} e^{-it_p^{(\ell)}(H_S + H_{c(\ell)})}\right), \tag{45}$$

with the finite duration of the ℓ -th single-qubit pulse layer $t_p^{(\ell)} > 0$, see figure 6. First, we provide the average Hamiltonian for one conjugation with a single-qubit

pulse block to investigate the effect of the finite pulse duration.

Lemma IV.2. The approximation of $U(t\lambda_c)$ in first or-

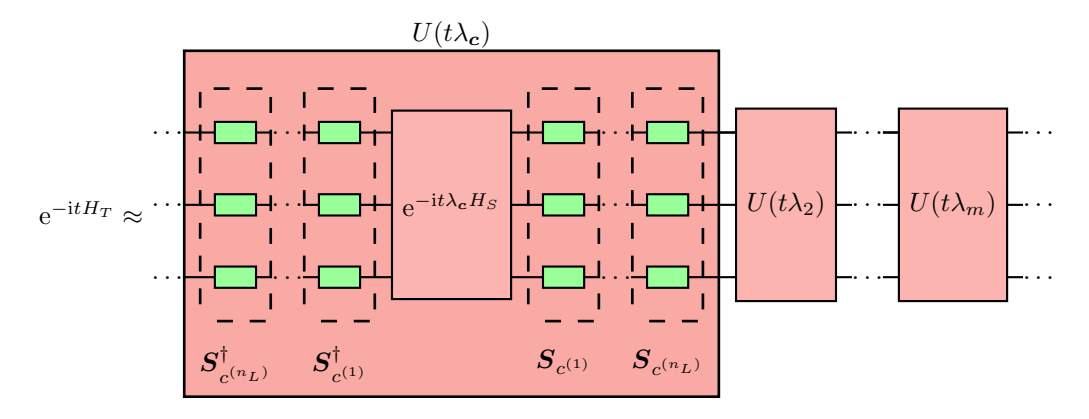


Figure 6. Exemplary quantum circuit for approximating the target evolution. We only implement simple single-qubit pulses in the presence of an always-on system Hamiltonian H_S .

der Magnus expansion is given by $e^{-iH_{av,c}(t)}$ with

$$H_{\text{av},\boldsymbol{c}}(t) = t\lambda_{\boldsymbol{c}} \boldsymbol{S}_{\boldsymbol{c}}^{\dagger} H_{S} \boldsymbol{S}_{\boldsymbol{c}} + H_{\text{err},\boldsymbol{c}}, \tag{46}$$

where

 H_{orr} a :=

$$2\sum_{\ell=1}^{n_L} \mathbf{S}_{\mathbf{c}^{\geq(\ell+1)}}^{\dagger} \int_0^{t_p^{(\ell)}} \mathbf{S}_{c^{(\ell)}}^{\dagger}(t) H_S \mathbf{S}_{c^{(\ell)}}(t) dt \, \mathbf{S}_{\mathbf{c}^{\geq(\ell+1)}}. \tag{47}$$

The average Hamiltonian $H_{av,c}(t)$ has the same interaction graph as H_S . Moreover, the error for truncating the Magnus expansion after the first order can be bounded in spectral norm by

$$||U(t\lambda_c) - e^{-iH_{av,c}(t)}|| \le O((2T_p + t\lambda_c)^2 ||H_S||^2).$$
 (48)

We define the matrices capturing the effect of the ideal evolution and the finite pulse time error to state a LP that cancels the finite pulse time error in the average Hamiltonian (in first order).

Lemma IV.3. Let $W(\mathbf{J})^{(r \times s)}$, $E(\mathbf{J})^{(r \times s)} \in \mathbb{R}^{r \times s}$ be the matrices representing the ideal conjugation and the finite pulse time error in the Pauli basis respectively. The entries are given by

$$W(\boldsymbol{J})_{\boldsymbol{a}\boldsymbol{c}}^{(r\times s)} := \frac{1}{2^n} \operatorname{Tr} \left(P_{\boldsymbol{a}} \left(\boldsymbol{S}_{\boldsymbol{c}}^{\dagger} H_S \boldsymbol{S}_{\boldsymbol{c}} \right) \right), \quad (49)$$

and

$$E(\boldsymbol{J})_{\boldsymbol{a}\boldsymbol{c}}^{(r\times s)} \coloneqq \frac{1}{2^n} \operatorname{Tr} \left(P_{\boldsymbol{a}} H_{\operatorname{err}, \boldsymbol{c}} \right) ,$$
 (50)

and can be calculated in polynomial time in the number of qubits for a local system Hamiltonian H_S .

The proofs of lemma IV.2 and lemma IV.3 can be found in appendix C. Let $W(\boldsymbol{J})^{(r\times s)}$ be feasible (as in definition III.1) and let $\sum_{\boldsymbol{c}} \lambda_{\boldsymbol{c}} \boldsymbol{S}_{\boldsymbol{c}}^{\dagger} H_{S} \boldsymbol{S}_{\boldsymbol{c}}$ be able to modify all interaction terms in the interaction graph of H_{S} . Then, the LP

minimize
$$\mathbf{1}^T \boldsymbol{\lambda}$$

subject to $W(\boldsymbol{J})^{(r \times s)} \boldsymbol{\lambda} + E(\boldsymbol{J})^{(r \times s)} \mathbf{1} = \boldsymbol{A}$,
 $\boldsymbol{\lambda} \in \mathbb{R}^s_{\geq 0}$ (robustLP)

always has a solution for any $A \in \mathbb{R}^r$. This follows directly from definition III.1. Now, we are ready to state the main result of this section.

Theorem IV.4. The target time evolution e^{-itH_T} can be efficiently approximated by a deterministic product formula implementing a product of $U(t\lambda_c)$, with λ_c from (robustLP). Moreover, this approximation is robust against the finite pulse time effect. The only approximation errors are given by the ones from the Magnus approximation (lemma IV.2) and the approximation error from the deterministic product formula.

Proof. The chosen product formula determines the number of implemented single-qubit conjugations $U(t\lambda_c)$ for each c. Let this number be n_c . The finite pulse time error term in (robustLP) has to be rescaled to account for n_c since each implementation of $U(t\lambda_c)$ causes the associated finite pulse time error. This can be done by multiplying the c-th column of $E(J)^{(r \times s)}$ by n_c .

For simplicity, we assume the first order Trotter approximation in eq. (31). To account for the number of implemented single-qubit conjugations we have to rescale $E(\boldsymbol{J})^{(r\times s)}$ by $n_{\boldsymbol{c}}=n_{\mathrm{Tro}}$ for all \boldsymbol{c} . Let $tH_{\mathrm{av}}\coloneqq\sum_{\boldsymbol{c}}^{s}H_{\mathrm{av},\boldsymbol{c}}(t)$, with $\lambda_{\boldsymbol{c}}$ from (robustLP). Let the target Hamiltonian be

$$H_T = \sum_{\boldsymbol{a} \in \mathbb{F}_2^{2n} \setminus \{\mathbf{0}\}} A_{\boldsymbol{a}} P_{\boldsymbol{a}}. \tag{51}$$

By the constraint of (robustLP), we have $H_{\text{av}} = H_T$. The time evolution governed by the target Hamiltonian H_T can be approximated with

$$e^{-itH_{T}} = e^{-itH_{av}}$$

$$\approx \left(\overrightarrow{\prod_{c}} e^{-iH_{av,c}\left(\frac{t}{n_{Tro}}\right)} \right)^{n_{Tro}}$$

$$\approx \left(\overrightarrow{\prod_{c}} U(t\lambda_{c}/n_{Tro}) \right)^{n_{Tro}},$$
(52)

where the first approximation is given by the Trotter scheme and the second approximation is given by the first order Magnus expansion from lemma IV.2. \Box

Remark 1. The Trotter approximation error can be bounded as in eq. (34) and depends on the evolution time $t \sum_{c} \lambda_{c}$. The approximation error for truncating the Magnus expansion increases with the finite pulse duration, see eq. (48). Note, that the truncation error bound in eq. (48) is not tight and might be improved [74].

Remark 2. The (robustLP) is efficiently solvable with the relaxation from section IIIB1 if $s \geq 2r$ with r the number of interaction terms that can be modified. To approximate the evolution under the target Hamiltonian H_T with n_{Tro} Trotter cycles we have to implement at most $n_{\text{Tro}}s$ evolution blocks $U(t\lambda_c)$, even if $\lambda_c = 0$. Since the finite pulse time errors for all single-qubit pulse layers are taken into account in (robustLP). Each evolution block contains $2n_L$ single-qubit pulse layers (possibly being part of a robust composite pulse sequence). Then, the total number of single-qubit pulse layers is at most $2n_L n_{\text{Tro}}s$.

The number of single-qubit pulse layers can be reduced by formulating the (MILP), which we explain in section IV E. This (MILP) reduces the number of evolution blocks in one Trotter cycle from $s \geq 2r$ to $s \approx r$. However, MILP's are in general hard to solve. The size of (MILP) is drastically reduced due to our efficient relaxation, and solving it for small instances is still feasible.

To summarize, our efficient relaxation plays a central role in both cases for solving the (robustLP) and (MILP). The (MILP) is feasible only for small instances whereas the (robustLP) is efficiently solvable at the cost of more single-qubit pulse layers.

In the next sections, we leverage the general robust conjugation method to robustify the Clifford and Pauli conjugation methods.

C. Robust Clifford conjugation method

For the Clifford conjugation method we have two single-qubit pulse layers $n_L=2$ of $\pi/2$ pulses, splitting the Pauli pulses into two pulses.

Definition IV.5 (Single-qubit Clifford pulse block). The single-qubit Clifford pulse block S_c is specified by the tuple $\mathbf{c} = ((t_p^{(1)}, \mathbf{s}^{(1)}, \mathbf{h}^{(1)}), (t_p^{(2)}, \mathbf{s}^{(2)}, \mathbf{h}^{(2)}))$, with the finite pulse times of one $\pi/2$ pulse, and we have $t_p^{(1)} = t_p^{(2)}$. The rotation direction $\mathbf{s}^{(\ell)}$ is fixed, and we set $\mathbf{s}_i^{(\ell)} = 1$ if on the i-th qubit and the ℓ layer we have $\sqrt{(\cdot)}^{\dagger}$ and $\mathbf{s}_i^{(\ell)} = 0$ if we have $\sqrt{(\cdot)}$. The generators are $h_i = \frac{\pi}{4t_p^{(\ell)}} P_i^{(\ell)}$, with the Pauli operators from the squareroot Pauli gates $P_i^{(\ell)}$.

The Clifford method can be made robust against the finite pulse time error by direct application of theorem IV.4. Our results for the efficient relaxation of the Clifford conjugation method in section III B 1 ensures that (robustLP) is feasible and that all interaction terms in the interaction graph of H_S can be modified.

Corollary IV.6 (Robustness against finite pulse time errors). Let there be two layers of $\pi/2$ pulses, representing the single-qubit pulses for the Clifford conjugation as in definition IV.5. Then, the finite pulse time effect can be suppressed using theorem IV.4.

The Clifford conjugation method can also be made robust by taking advantage of the rich field of robust composite pulses. The $\pi/2$ pulses in each of the two layers in the Clifford conjugation method can be made robust by replacing each pulse with robust composite pulses of length $n_L/2$. Then, the finite pulse time error is different but can still be corrected using theorem IV.4.

Corollary IV.7 (Robustness against pulse errors). Let there be a robust composite pulse sequence for $\pi/2$ pulses of length $n_L/2$. Replacing each $\pi/2$ pulse in the Clifford conjugation method by such robust composite pulses yields n_L single-qubit pulse layers. Then, the finite pulse time effect is different from corollary IV.6 but still can be suppressed by theorem IV.4.

The ability to modify any interaction in the interaction graph of H_S and the combination with robust composite pulses makes our Clifford conjugation robust against a wide range of different errors in experiments. Note, that composite pulses with a short overall duration are more beneficial due to the faster convergence of the Magnus expansion eq. (40). In section VB we combine the SCROFULOUS pulses [75] and the SCROBUTUS pulses [61] with the robust Clifford conjugation to implement arbitrary Heisenberg Hamiltonians.

D. Robust Pauli conjugation method

The Pauli conjugation can only change the Pauli coefficients in the system Hamiltonian but not modify the type of interactions. Consequently, the general robust conjugation method is not directly applicable. Therefore, we generalize the robustness conditions of Votto et al. [18] to arbitrary local Hamiltonians.

Definition IV.8 (Single-qubit Pauli pulse layer). The single-qubit Pauli pulse layer S_c is specified by the tuple $c = (t_p, s, h)$, with the finite pulse time t_p of one π pulse. The rotation direction is $s \in \mathbb{F}_2^n$ and can be chosen freely for π pulses. The generators are $h_i = \frac{\pi}{2}P_i$, with the Pauli operator P_i given by P_{b_i} from eq. (11).

For the Pauli conjugation $U(t\lambda_c)$ simplifies to

$$U(t\lambda_{\mathbf{c}}) = e^{-it_p(H_S - H_{\mathbf{c}})} e^{-it\lambda_{\mathbf{c}}H_S} e^{-it_p(H_S + H_{\mathbf{c}})}.$$
 (53)

Next, we provide the average Hamiltonian for the conjugation of the system Hamiltonian with a single-qubit Pauli pulse layer to investigate the effect of the finite pulse time.

Lemma IV.9. Consider all labels $\mathbf{a} \in \mathbb{F}_2^{2n}$ for the non-zero interactions $J_{\mathbf{a}} \neq 0$ in the system Hamiltonian.

Then, the approximation of $U(t\lambda_{\mathbf{c}})$ for the Pauli conjugation in first order Magnus expansion is given by $e^{-iH_{\mathrm{av},\mathbf{c}}(t)}$ with

$$H_{\text{av},\boldsymbol{c}}(t) = t\lambda_{\boldsymbol{c}} S_{\boldsymbol{c}}^{\dagger} H_{S} S_{\boldsymbol{c}} + H_{\text{err},\boldsymbol{c}}, \qquad (54)$$

where

$$H_{\text{err},c} = \sum_{\boldsymbol{a} \in \mathbb{F}_2^{2n} \setminus \{0\}} \left(J_{\boldsymbol{a}} E_{\boldsymbol{a},c}^{(r \times s)} P_{\boldsymbol{a}} + R_{\boldsymbol{a},c} \right).$$
 (55)

We call the first term in eq. (55) the interaction term, with

$$E_{\boldsymbol{a},\boldsymbol{c}}^{(r\times s)} := \frac{4t_p}{\pi} \int_0^{\frac{\pi}{2}} \left(\prod_{i \in \text{supp}(\boldsymbol{a})} (\cos^2(\theta) + (-1)^{\langle \boldsymbol{a}_i, \boldsymbol{b}_i \rangle} \sin^2(\theta)) \right) d\theta,$$
(56)

which we collect as entries of the matrix $E^{(r \times s)} \in \mathbb{R}^{r \times s'}$. We call the second term $R_{\mathbf{a},\mathbf{c}}$ the rest term, and it is proportional to $(-1)^{\mathbf{e}_{\mathbf{a}} \cdot \mathbf{s}}$, with $\mathbf{s} \in \mathbb{F}_2^n$ representing the chosen rotation direction of the π pulses and $\mathbf{e}_{\mathbf{a}} \in \mathbb{F}_2^n$ encodes the sign flips due to the finite pulse time error such that $\mathbf{e}_{\mathbf{a},i} = 0$ for all $i \notin \operatorname{supp}(\mathbf{a})$.

All proofs in this section can be found in appendix D. We define the LP similar to (robustLP)

(robustPauliLP)

with $W^{(r\times s)} \in \mathbb{R}^{r\times s}$ and $M \in \mathbb{R}^r$ from section III A and $E^{(r\times s)} \in \mathbb{R}^{r\times s}$ from lemma IV.9. Similar to theorem IV.4 we can cancel the effect of the interaction terms in eq. (55) by implementing $U(t\lambda_c)$, with λ_c from (robustPauliLP). However, there still remains the rest terms $R_{a,c}$ in eq. (55) which can be cancelled by selecting the π pulse direction appropriately.

Proposition IV.10 (Robustness against finite pulse time errors). The target time evolution e^{-itH_T} can be approximated by a deterministic product formula implementing $U(t\lambda_c)$, with λ_c from (robustPauliLP), and choosing the rotation directions $s \in \mathbb{F}_2^n$ of the π pulses such that $\sum_s (-1)^{e_a \cdot s} = 0$ for all $e_a \in \mathbb{F}_2^n$ with $e_{a,i} = 0$ for all $i \notin \text{supp}(a)$ for any a with $J_a \neq 0$, as in lemma IV.9. The only approximation errors are given by the ones from the Magnus approximation (lemma IV.2) and the approximation error from the deterministic product formula.

Proof. Similar as in the proof of theorem IV.4 the columns of $E^{(r\times s)}$ in (robustPauliLP) has to be rescaled by the number of implementations $U(t\lambda_c)$ which we denote by n_c . For simplicity we assume the first order Trotter approximation in eq. (31).

We start with the rest term in the average Hamiltonian in eq. (55) which is proportional to $(-1)^{e_a \cdot s}$.

Let's assume we require κ different rotation directions $s_{(1)},\ldots,s_{(\kappa)}\in\mathbb{F}_2^n$ such that $\sum_{j=1}^{\kappa}(-1)^{e_{\boldsymbol{a}}\cdot s_{(j)}}=0$ for all $e_{\boldsymbol{a}}\in\mathbb{F}_2^n$ with $e_{\boldsymbol{a},i}=0$ for all $i\notin \operatorname{supp}(\boldsymbol{a})$ for any \boldsymbol{a} with $J_{\boldsymbol{a}}\neq 0$. A non-optimal choice of $s_{(j)}$ are all possible binary combinations without the all-zero vector, then $\kappa=2^n-1$. An efficient choice is provided in proposition IV.12 below. To indicate the used rotation direction, we specify the single-qubit Pauli pulse layer by the tuple $c_{(j)}=(t_p,s_{(j)},h)$. Note, that the generators do not change. Let the partial average Hamiltonian be the average Hamiltonian without the rest error term

$$\tilde{H}_{\text{av},\mathbf{c}}(t) \coloneqq \sum_{j=1}^{\kappa} H_{\text{av},\mathbf{c}_{(j)}} \left(\frac{t}{\kappa}\right)
= t\lambda_{\mathbf{c}} \mathbf{S}_{\mathbf{c}}^{\dagger} H_{S} \mathbf{S}_{\mathbf{c}} + \kappa \sum_{\mathbf{a} \in \mathbb{F}_{2}^{2n} \setminus \{\mathbf{0}\}} E_{\mathbf{a},\mathbf{c}}^{(r \times s)} J_{\mathbf{a}} P_{\mathbf{a}}.$$
(57)

The evolution under the partial average Hamiltonian can be approximated by

$$e^{-it\tilde{H}_{av,c}(t)} \approx \prod_{j=1}^{\kappa} e^{-iH_{av,c_{(j)}}(\frac{t}{\kappa})} \approx \prod_{j=1}^{\kappa} U(t\lambda_{c_{(j)}}/\kappa), (58)$$

where the first approximation is given by a first order Trotter scheme where we set $n_{\rm Tro}=1$ for simplicity, and the second approximation is given by the first order Magnus expansion from lemma IV.2. Let $tH_{\rm av} := \sum_c^s \tilde{H}_{\rm av,c}(t)$, with λ_c from (robustPauliLP). Let the target Hamiltonian be

$$H_T = \sum_{\boldsymbol{a} \in \mathbb{F}_2^{2n} \setminus \{\boldsymbol{0}\}} A_{\boldsymbol{a}} P_{\boldsymbol{a}}. \tag{59}$$

By the constraint of (robustPauliLP), we have $H_{\text{av}} = H_T$. The time evolution governed by the target Hamiltonian H_T can be approximated with

$$e^{-itH_{T}} = e^{-itH_{av}}$$

$$\approx \left(\overrightarrow{\prod_{c}} e^{-i\widetilde{H}_{av,c_{(j)}} \left(\frac{t}{n_{Tro}} \right)} \right)^{n_{Tro}}$$

$$\approx \left(\overrightarrow{\prod_{c}} \overrightarrow{\prod_{j=1}^{\kappa}} U \left(\frac{t\lambda_{c_{(j)}}}{\kappa n_{Tro}} \right) \right)^{n_{Tro}}, \tag{60}$$

where the first approximation is given by the Trotter scheme. To account for the number of implemented Pauli conjugations $U(t\lambda_c)$ we have to rescale $E^{(r\times s)}$ by $n_c = \kappa n_{\text{Tro}}$ for all c.

Note, that even if $\lambda_c = 0$ the evolution block $U(t\lambda_c)$ still has to be implemented with zero free evolution time. The number of evolution blocks can be reduced by formulating a MILP, which we explain in section IV E.

The robustness against finite pulse time errors simultaneously implies robustness against the first order effects of rotation angle errors.

Proposition IV.11. Let the rotation directions $\mathbf{s} \in \mathbb{F}_2^n$ of the π pulses such that $\sum_{\mathbf{s}} (-1)^{\mathbf{e_a} \cdot \mathbf{s}} = 0$ for all $\mathbf{e_a} \in \mathbb{F}_2^n$ with $\mathbf{e_{a,i}} = 0$ for all $i \notin \text{supp}(\mathbf{a})$ for any \mathbf{a} with $J_{\mathbf{a}} \neq 0$, as in lemma IV.9. Then, the rotation angle errors in the first order Taylor approximation cancels.

Given a system Hamiltonian with only two-body interactions, i.e. only interactions P_a with $|\operatorname{supp}(a)| = 2$, a good choice for the π pulse rotation directions $s_{(j)} \in \mathbb{F}_2^n$ for $j = 1, \ldots, \kappa$ can be found by utilizing the orthogonality property of Walsh-Hadamard matrices.

Proposition IV.12. Let $\kappa = 2^{\lceil \log_2(n+1) \rceil} \leq 2n$ and let $W^{(\kappa \times \kappa)}$ be the $\kappa \times \kappa$ dimensional Walsh-Hadamard matrix. Choose n distinct columns from $W^{(\kappa \times \kappa)}$ without the first column and define the resulting partial Walsh-Hadamard matrix as $W^{(\kappa \times n)}$. Let $(-1)^{s_{(j)}}$ be the j-th row of $W^{(\kappa \times n)}$. Then, for $\mathbf{a} \in \mathbb{F}_2^{2n}$ and $\mathbf{e}_{\mathbf{a}} \in \mathbb{F}_2^n$ with $|\sup_{j=1}^{\kappa} (-1)^{e_{\mathbf{a}} \cdot s_{(j)}} = 0$.

E. Reducing the number of single-qubit pulses

Let W, E be either $W(\boldsymbol{J})^{(r \times s)}, E(\boldsymbol{J})^{(r \times s)}$ or $W^{(r \times s)}, E^{(r \times s)}$ as in (robustLP) or (robustPauliLP) respectively. In these LPs the sum of the finite pulse time effects for all considered evolution blocks $U(t\lambda_c)$ is given by the vector $E \cdot \mathbf{1} \in \mathbb{R}^r$. The solution λ in the (robustLP) and (robustPauliLP) is sparse [41]. However, when mitigating the finite pulse time errors as in theorem IV.4 and proposition IV.10 then all the single-qubit pulse conjugations have to be implemented (with zero free evolution time if $\lambda_c = 0$). The LP's can be extended with additional binary variables $z \in \{0,1\}^s$ and an additional constraint to only consider the finite pulse time errors for the single-qubit pulses with non-zero free evolution time [76]. This yields the mixed integer linear program (MILP)

minimize
$$\alpha \mathbf{1}^{T} \boldsymbol{\lambda} + (1 - \alpha) \mathbf{1}^{T} \boldsymbol{z}$$

subject to $W \boldsymbol{\lambda} + E \boldsymbol{z} = \boldsymbol{M}$,
 $c_{l} \boldsymbol{z} \leq \boldsymbol{\lambda} \leq c_{u} \boldsymbol{z}$,
 $\boldsymbol{\lambda} \in \mathbb{R}^{s}_{\geq 0}$, $\boldsymbol{z} \in \{0, 1\}^{s}$. (MILP)

The free parameter $\alpha \in [0,1]$ assigns weights to the minimization of the free evolution times $\alpha = 1$ or the minimization of the number of single-qubit pulse layers $\alpha = 0$. $0 \le c_l < c_u$ are lower and upper bounds on the entries of λ . The interval $[c_l, c_u]$ has to be large enough such that (MILP) has a solution. Although (MILP) is in general hard to solve, there are many powerful heuristics and software packages to solve such optimizations [48].

If not otherwise stated, we used the parameters $c_l=10^{-6},\,c_u=10^3$ and $\alpha=10^{-2}.$ We used MOSEK to solve (MILP) with parameter MSK_DPAR_MIO_TOL_REL_GAP set to 1.0 [48].

V. NUMERICAL HAMILTONIAN SIMULATIONS

To benchmark our methods, we perform numerical simulations that model the most relevant error sources occurring in practice. We consider a device with 2D lattice interactions, motivated by superconducting qubit platforms, and one with all-to-all connectivity modelling an ion trap. However, the presented methods are also applicable to other platforms such as cold atoms.

We numerically simulate the time evolution given by the robust Pauli and Clifford conjugation methods by explicitly computing products of matrix exponentials. More precisely, the decomposition of the target Hamiltonian is implemented using the first- or second-order Trotter formula,

$$U_{\rm sim} = \left(\overrightarrow{\prod_{c}} U \left(\frac{t \lambda_{c}}{n_{\rm Tro}} \right) \right)^{n_{\rm Tro}}$$
 (61)

Ol

$$U_{\rm sim} = \left(\prod_{c} U \left(\frac{t \lambda_c}{2n_{\rm Tro}} \right) \prod_{c} U \left(\frac{t \lambda_c}{2n_{\rm Tro}} \right) \right)^{n_{\rm Tro}}, \quad (62)$$

where a single evolution block $U(t\lambda_c)$ consists of the time evolution under the system Hamiltonian conjugated by single-qubit pulses as in eq. (45), and thus explicitly models finite pulse time errors.

We model the rotation angle and off-resonance errors of one single-qubit pulse layer, similar to definition IV.1, as

$$H_{c,(\varepsilon,f)} = \frac{1}{t_p} \sum_{i=1}^{n} ((1+\varepsilon_i)(-1)^{s_i} h_i + f_i Z_i) , \qquad (63)$$

where $\varepsilon_i \overset{\text{i.i.d.}}{\sim} \text{unif}([0,\varepsilon])$ is the relative angle error and $f_i \overset{\text{i.i.d.}}{\sim} \text{unif}([0,f])$ is the off-resonance error on the *i*-th qubit. The relative angle error is sampled once and represents faulty and inhomogeneous control of the single-qubit pulses.

To capture the quality of the implementation, U_{sim} is compared to the target evolution $U_T = e^{-itH_T}$. As a measure of quality, we use the average gate infidelity

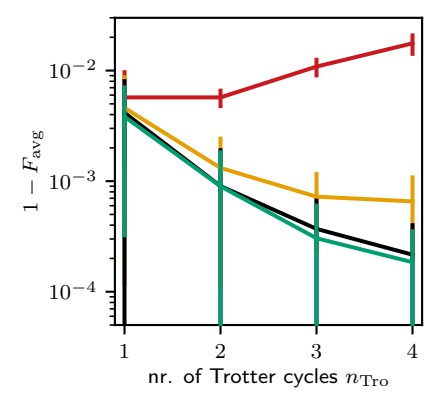
$$1 - F_{\text{avg}}(U_{\text{sim}}, U_T) = 1 - \frac{\text{Tr}(U_T^{\dagger} U_{\text{sim}}) + 1}{d+1}, \quad (64)$$

with the Hilbert space dimension d.

A. Simulation of a 2D lattice model

We consider a quantum platform with a native 2×3 lattice Hamiltonian with n=6 qubits as an abstract model for interacting superconducting qubits,

$$H_S = J \sum_{ij} Z_i Z_j + \sum_{ijk} E_{ijk} X_i X_j X_k. \tag{65}$$



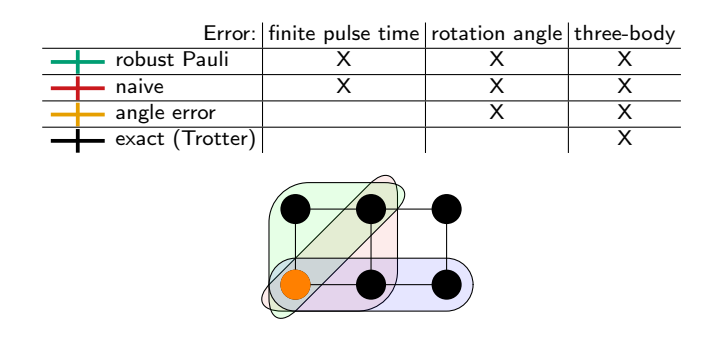


Figure 7. Left: The sample mean and standard deviation of the average gate infidelities eq. (64) for implementing the time evolution of e^{-itH_T} with H_T from eq. (66) and t=1s over the number of Trotter cycles n_{Tro} is shown. The sample mean and standard deviation are calculated over 50 random samples of the target Hamiltonians H_T . Note, that each Trotter cycle contains $\kappa=8$ evolution blocks $U(t\lambda_c)$ with different rotation directions for the π pulses. Top Right: Table indicating which error types are present for the different simulations. Bottom right: Example 2×3 2D square lattice on n=6 qubits with the two-body interactions, solid black lines, and the three-body interactions for the lower left qubit, colored areas.

We assume that there are unwanted three-body interactions of unknown strength, where we consider all possible nearest neighbor three-body interactions. An example of the considered two- and three-body interactions are depicted in figure 7 as solid black lines and colored areas respectively. The two-body coupling coefficients are constant, $J=10^3\,\mathrm{Hz}$. The three-body coupling coefficients are uniformly sampled $E_{ijk} \stackrel{\mathrm{i.i.d.}}{\sim} \mathrm{unif}([-10^2,10^2]\cdot\mathrm{Hz})$ after the design of the pulse sequences and therefore considered as unknown. The finite π pulse time is $t_p=10^{-7}\,\mathrm{s.}$ We want to implement the Ising Hamiltonian

$$H_T = \sum_{ij} A_{ij} Z_i Z_j , \qquad (66)$$

with coupling coefficients $A_{ij} \stackrel{\text{i.i.d.}}{\sim} \text{unif}([10^{-1}, 1] \cdot \text{Hz})$. The pulse errors are modeled as in eq. (63) with $\varepsilon = 10^{-1}$ and no off-resonance error.

In figure 7 we compare the naive Pauli conjugation from section III A to the robust Pauli conjugation from section IVD to generate the target Hamiltonian H_T . For the robust Pauli conjugation the relative evolution times λ are the solutions of the (MILP) for the (robustPauliLP). We use the π pulse rotation directions as in proposition IV.12, canceling all two-body terms in the average Hamiltonian. Therefore, for n = 6 qubits $\kappa = 2^{\lceil \log_2(n+1) \rceil} = 8$ different rotation directions are required. To cancel the unwanted and unknown threebody interaction terms we apply the results from section IIIC to both approaches. In the angle error and exact (Trotter) data we apply the same sequences as for the naive but with different errors, see table in figure 7. To approximate the time evolution under H_T we use the first-order Trotter formula from eq. (61) for all sequences. Increasing the number of Trotter cycles n_{Tro} improves the accuracy of the Trotter approximation in absence of other errors. However, an increased number of Trotter cycles $n_{\rm Tro}$ also yields an increased number of evolution blocks $U(t\lambda_c)$. From figure 7 it is clear that the finite pulse time errors and angle errors in the naive sequences quickly accumulate even for small number of Trotter cycles. However, the robust Pauli sequences converge as quickly as the Trotter sequences without any errors.

B. Simulation of Heisenberg Hamiltonians with an ion trap model

We consider an ion trap with Ytterbium ions in an external magnetic field gradient [77]. The effective system Hamiltonian is

$$H_S = \sum_{i \neq j}^n J_{ij} Z_i Z_j \,, \tag{67}$$

where the coupling coefficients J_{ij} are calculated for a harmonic trapping potential affecting the equilibrium positions of the ions in the magnetic field gradient (cf. Ref. [36, App. A]). We consider all-to-all connectivity, thus the number of reachable interactions is $r = \frac{n}{2}(n-1)$ for the Pauli conjugation and $r = 3^2 \frac{n}{2}(n-1)$ for the Clifford conjugation. The coupling coefficients J_{ij} are proportional to $(B_1/\omega)^2$, with a magnetic field gradient of $B_1 = 40 \, T/m$ and a trap frequency of $\omega = 2\pi 500 \, k$ Hz. The finite π pulse time is $t_p = 2 \, \mu$ s, which is proportional to π/Ω with the Rabi frequency $\Omega = \omega/2$. Moreover, we consider the rotation angle errors of strength $\varepsilon = 10^{-1}$ and off-resonance errors of strength $f = 10^{-1}$, which are modeled as in eq. (63).

As a target Hamiltonian, we consider the general Heisenberg Hamiltonian

$$H_T = \sum_{i \neq j}^n \left(A_{ij}^x X_i X_j + A_{ij}^y Y_i Y_j + A_{ij}^z Z_i Z_j \right) , \qquad (68)$$

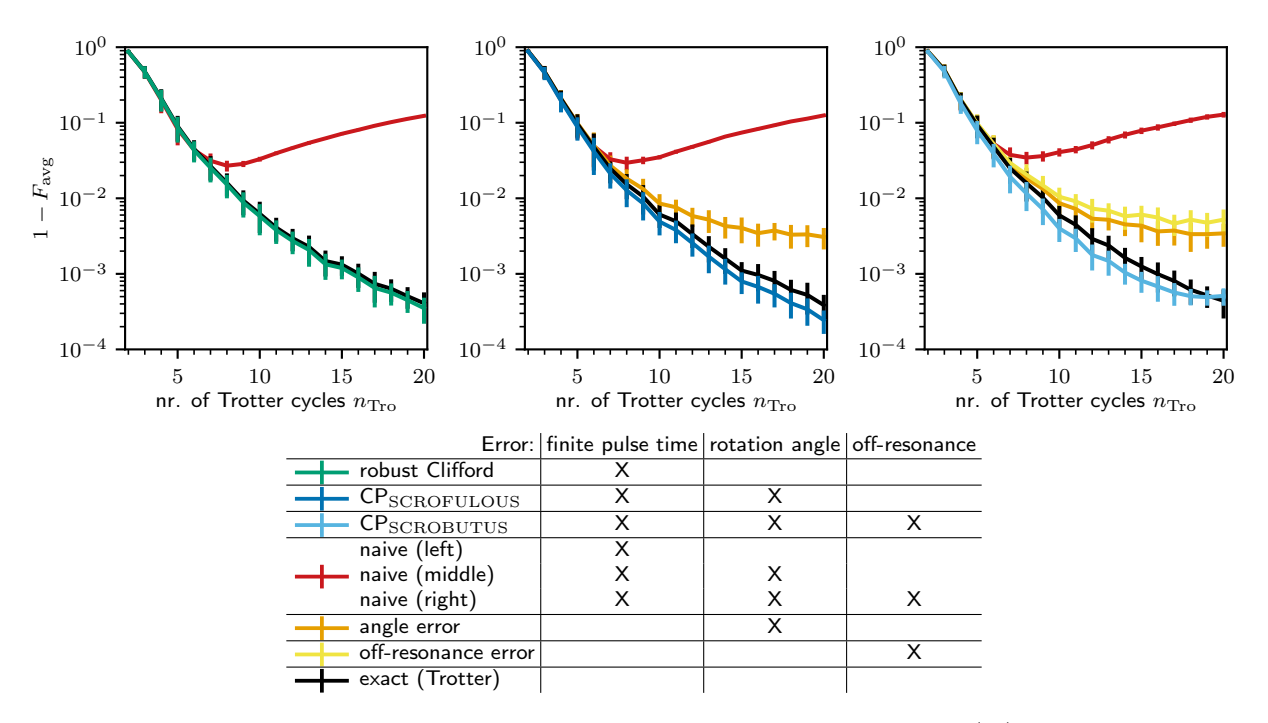


Figure 8. Top: The sample mean and standard deviation of the average gate infidelities eq. (64) for implementing the time evolution of e^{-itH_T} with H_T from eq. (68) and $t=1\,sec$ over the number of Trotter cycles $n_{\rm Tro}$ is shown. The sample mean and standard deviation are calculated over 50 random samples of the Heisenberg Hamiltonians H_T on n=8 qubits. Top Left: The Clifford conjugation robust against finite pulse time errors (dark green) is compared to the non-robust Clifford conjugation (red). Top Middle: The Clifford conjugation in combination with the SCROFULOUS pulse sequence [75] robust against finite pulse time errors and rotation angle errors (dark blue) is compared to the non-robust Clifford conjugation (red). Top Right: The Clifford conjugation in combination with the SCROBUTUS pulse sequence [61] robust against finite pulse time errors, rotation angle errors and off-resonance errors (light blue) is compared to the non-robust Clifford conjugation (red). Bottom: Table indicating which error types are present for the different simulations.

with coupling coefficients $A^x_{ij}, A^y_{ij}, A^z_{ij} \overset{\text{i.i.d.}}{\sim} \text{unif}([10^{-1}, 1] \cdot \text{Hz})$ and all-to-all connectivity.

In figure 8 we compare the naive Clifford conjugation from section IIIB to the robust Clifford, CP_{SCROFULOUS} and CP_{SCROBUTUS} Clifford conjugations from section IVC to generate the target Hamiltonian H_T . The robust Clifford method is robust against the finite pulse time error. The $\mathsf{CP}_{\mathsf{SCROFULOUS}}$ method is additionally robust against rotation angle errors. It is given as a combination of our robust Clifford conjugation with the SCROFULOUS composite pulses [75]. Finally, the CP_{SCROBUTUS} method is robust against the finite pulse time error, rotation angle errors and off-resonance errors. It is given as a combination of our robust Clifford conjugation with the SCROBUTUS composite pulses [61]. For the robust Clifford, CP_{SCROFULOUS} and CP_{SCROBUTUS} Clifford conjugation the relative evolution times λ are the solutions of the (MILP) version of (robustLP). For the angle error, off-resonance error and exact (Trotter) data we apply the same sequences as for the naive data but with different errors, see table in figure 8. To approximate the time evolution under H_T we use the secondorder Trotter formula from eq. (62) for all sequences. As for the Pauli conjugation method in section VA, we can observe that the finite pulse time errors and angle errors in the naive sequences quickly accumulate even for moderate number of Trotter cycles. However, the robust Clifford, $\mathsf{CP}_{\mathsf{SCROFULOUS}}$ and $\mathsf{CP}_{\mathsf{SCROBUTUS}}$ sequences converge as quickly as the Trotter sequences without any errors, and seem to be even more accurate at moderate numbers of Trotter cycles.

Note, that the rotation angle error robustness in the $\mathsf{CP}_{\mathsf{SCROFULOUS}}$ Clifford conjugation is stronger than in the robust Pauli conjugation in section V A. Since each $\pi/2$ pulse (replaced by robust composite pulses) is robust against different angle errors whereas in the robust Pauli conjugation the angle errors are assumed to be constant over several implementations of $U(t\lambda_c)$.

VI. DISCUSSION AND OUTLOOK

We consider a quantum computing or quantum simulation platform that has one single entangling Hamiltonian as system Hamiltonian and provide efficient, general and robust methods to engineer arbitrary local Hamiltonians with the same interaction graph from it. Our methods only rely on the use of Pauli or single-qubit Clifford gates and explicitly allows for robust composite pulses. They can be directly used in experiments by applying the pulse sequences generated by the provided Python code [49].

The pulse sequences for the single-qubit gates are obtained by solving a suitable linear program (LP), the classical runtime of which depends polynomially only on the number of Pauli terms in the system Hamiltonian and its interaction graph and can thus be efficiently solved for local Hamiltonians. The Pauli conjugation method is even applicable if only partial knowledge of the system Hamiltonian is available, and can be used to cancel unwanted, but unknown interaction terms. Moreover, the quantum simulation runtime can be reduced at the cost of a higher classical runtime, which provides a flexible trade-off.

Another major advantage of our methods is the robustness against experimental imperfections. Simulation errors introduced by finite pulse times can be explicitly compensated in the computation of the pulse sequence. The Clifford conjugation method can be combined with robust composite pulses, making it robust against major experimental errors. We discuss in detail the effect of finite pulse time errors and rotation angle errors and show that these can be fully mitigated by modified pulse sequences in combination with robust composite pulses. Due to their generality and efficiency, we expect that our methods will find many applications in quantum computation and quantum simulation, such as the fast synthesis of multi-qubit gates, or analogue quantum simulation for problems arising in many-body physics. Furthermore, some recent Hamiltonian learning schemes rely on "reshaping" an unknown Hamiltonian to a diagonal Hamiltonian which can be done efficiently and in a robust way with our Pauli conjugation method [33–35].

In the future, we would like to extend the efficient

Hamiltonian engineering method to fermionic systems for digital and analogue quantum simulations. Another promising future research direction could be the investigation of finite pulse time effects for continuous robust pulses similar to section IVB. Moreover, the design of robust pulses tailored to the conjugation methods might be another interesting direction.

ACKNOWLEDGEMENTS

We are grateful to Ivan Boldin, Patrick Huber, Markus Nünnerich and Rodolfo Muñoz Rodriguez for a productive dialogue on the ion trap platform, and to Matthias Zipper and Christopher Cedzich for fruitful discussions on gate designs for ion trap platforms. Moreover, we thank Matteo Votto for a constructive exchange about his impressive work and the robust sequences therein. We also thank Gaurav Bhole for making us aware of his results. Furthermore, we want to thank Özgün Kum for invaluable comments on our manuscript.

This work has been funded by the German Federal Ministry of Education and Research (BMBF) within the funding program "Quantum Technologies – from Basic Research to Market" via the joint project MIQRO (grant number 13N15522); the ERDF of the European Union and by Fonds of the Hamburg Ministry of Science, Research, Equalities and Districts (BWFGB); and the Fujitsu Services GmbH as part of the endowed professorship "Quantum Inspired and Quantum Optimization."

R. Somma, G. Ortiz, J. E. Gubernatis, E. Knill, and R. Laflamme, Simulating physical phenomena by quantum networks, Phys. Rev. A 65, 042323 (2002), arXiv:quant-ph/0108146.

^[2] R. Blatt and C. F. Roos, Quantum simulations with trapped ions, Nat. Phys. 8, 277 (2012).

^[3] D. Wecker, M. B. Hastings, N. Wiebe, B. K. Clark, C. Nayak, and M. Troyer, Solving strongly correlated electron models on a quantum computer, Phys. Rev. A 92, 062318 (2015), arXiv:1506.05135.

^[4] H. Bernien, S. Schwartz, A. Keesling, H. Levine, A. Omran, H. Pichler, S. Choi, A. S. Zibrov, M. Endres, M. Greiner, V. Vuletić, and M. D. Lukin, *Probing many-body dynamics on a 51-atom quantum simulator*, Nature 551, 579 (2017), arXiv:1707.04344.

^[5] J. Zhang, G. Pagano, P. W. Hess, A. Kyprianidis, P. Becker, H. Kaplan, A. V. Gorshkov, Z.-X. Gong, and C. Monroe, Observation of a many-body dynamical phase transition with a 53-qubit quantum simulator, Nature 551, 601 (2017), arXiv:1708.01044.

^[6] N. Defenu, A. Lerose, and S. Pappalardi, Out-ofequilibrium dynamics of quantum many-body systems with long-range interactions, Physics Reports 1074, 1 (2024), arXiv:2307.04802.

^[7] I. Kassal, J. D. Whitfield, A. Perdomo-Ortiz, M.-H. Yung, and A. Aspuru-Guzik, Simulating chemistry using

quantum computers, Annual Review of Physical Chemistry **62**, 185 (2011), arXiv:1007.2648.

^[8] D. Wecker, B. Bauer, B. K. Clark, M. B. Hastings, and M. Troyer, Gate-count estimates for performing quantum chemistry on small quantum computers, Phys. Rev. A 90, 022305 (2014), arXiv:1312.1695.

^[9] J. Olson, Y. Cao, J. Romero, P. Johnson, P.-L. Dallaire-Demers, N. Sawaya, P. Narang, I. Kivlichan, M. Wasielewski, and A. Aspuru-Guzik, *Quantum information and computation for chemistry*, arXiv:1706.05413 (2017).

^[10] A. M. Childs, D. Maslov, Y. Nam, N. J. Ross, and Y. Su, Toward the first quantum simulation with quantum speedup, Proceedings of the National Academy of Sciences 115, 9456 (2018), arXiv:1711.10980.

^[11] A. J. Daley, I. Bloch, C. Kokail, S. Flannigan, N. Pearson, M. Troyer, and P. Zoller, *Practical quantum advantage in quantum simulation*, Nature 607, 667 (2022).

^[12] J. Preskill, Quantum Computing in the NISQ era and beyond, Quantum 2, 79 (2018), arXiv:1801.00862.

^[13] R. Trivedi, A. Franco Rubio, and J. I. Cirac, Quantum advantage and stability to errors in analogue quantum simulators, Nature Communications 15, 6507 (2024), arXiv:2212.04924.

^[14] D. W. Leung, I. L. Chuang, F. Yamaguchi, and Y. Yamamoto, Efficient implementation of coupled logic gates

- for quantum computation, Phys. Rev. A **61**, 042310 (2000), arXiv:quant-ph/9904100.
- [15] D. Leung, Simulation and reversal of n-qubit Hamiltonians using Hadamard matrices, Journal of Modern Optics 49, 1199 (2002), arXiv:quant-ph/0107041.
- [16] J. L. Dodd, M. A. Nielsen, M. J. Bremner, and R. T. Thew, Universal quantum computation and simulation using any entangling Hamiltonian and local unitaries, Phys. Rev. A 65, 040301 (2002), arXiv:quantph/0106064.
- [17] M. A. Nielsen, M. J. Bremner, J. L. Dodd, A. M. Childs, and C. M. Dawson, Universal simulation of Hamiltonian dynamics for quantum systems with finite-dimensional state spaces, Phys. Rev. A 66, 022317 (2002), arXiv:quant-ph/0109064.
- [18] M. Votto, J. Zeiher, and B. Vermersch, Universal quantum processors in spin systems via robust local pulse sequences, Quantum 8, 1513 (2024), arXiv:2311.10600.
- [19] J. Choi, H. Zhou, H. S. Knowles, R. Landig, S. Choi, and M. D. Lukin, Robust dynamic Hamiltonian engineering of many-body spin systems, Phys. Rev. X 10, 031002 (2020), arXiv:1907.03771.
- [20] S. Choi, N. Y. Yao, and M. D. Lukin, Dynamical engineering of interactions in qudit ensembles, Phys. Rev. Lett. 119, 183603 (2017), arXiv:1703.09808.
- [21] H. Zhou, H. Gao, N. T. Leitao, O. Makarova, I. Cong, A. M. Douglas, L. S. Martin, and M. D. Lukin, Robust Hamiltonian engineering for interacting qudit systems, Phys. Rev. X 14, 031017 (2024), arXiv:2305.09757.
- [22] S. Geier, N. Thaicharoen, C. Hainaut, T. Franz, A. Salzinger, A. Tebben, D. Grimshandl, G. Zürn, and M. Weidemüller, Floquet Hamiltonian engineering of an isolated many-body spin system, Science 374, 1149 (2021), arXiv:2105.01597.
- [23] H. Zhou, J. Choi, S. Choi, R. Landig, A. M. Douglas, J. Isoya, F. Jelezko, S. Onoda, H. Sumiya, P. Cappellaro, H. S. Knowles, H. Park, and M. D. Lukin, *Quantum metrology with strongly interacting spin systems*, Phys. Rev. X 10, 031003 (2020), arXiv:1907.10066.
- [24] M. Garcia-de Andoin, A. Saiz, P. Pérez-Fernández, L. Lamata, I. Oregi, and M. Sanz, Digital-analog quantum computation with arbitrary two-body Hamiltonians, Phys. Rev. Res. 6, 013280 (2024), arXiv:2307.00966.
- [25] D. Hayes, S. T. Flammia, and M. J. Biercuk, Programmable quantum simulation by dynamic Hamiltonian engineering, New J. Phys. 16, 10.1088/1367-2630/16/8/083027 (2014), arXiv:1309.6736.
- [26] C. Figgatt, A. Ostrander, N. M. Linke, K. A. Landsman, D. Zhu, D. Maslov, and C. Monroe, Parallel entangling operations on a universal ion-trap quantum computer, Nature 572, 368 (2019), arXiv:1810.11948.
- [27] Y. Lu, S. Zhang, K. Zhang, W. Chen, Y. Shen, J. Zhang, J.-N. Zhang, and K. Kim, Global entangling gates on arbitrary ion qubits, Nature 572, 363 (2019), arXiv:1901.03508.
- [28] N. Grzesiak, R. Blümel, K. Wright, K. M. Beck, N. C. Pisenti, M. Li, V. Chaplin, J. M. Amini, S. Debnath, J.-S. Chen, and Y. Nam, Efficient arbitrary simultaneously entangling gates on a trapped-ion quantum computer, Nat. Commun. 11, 2963 (2020), arXiv:1905.09294.
- [29] J. K. Pachos and M. B. Plenio, Three-spin interactions in optical lattices and criticality in cluster Hamiltonians, Phys. Rev. Lett. 93, 056402 (2004), arXiv:quantph/0401106.
- [30] H. P. Büchler, A. Micheli, and P. Zoller, Three-body in-

- teractions with cold polar molecules, Nature Physics 3, 726 (2007), arXiv:cond-mat/0703688.
- [31] X. Peng, J. Zhang, J. Du, and D. Suter, Quantum simulation of a system with competing two- and threebody interactions, Phys. Rev. Lett. 103, 140501 (2009), arXiv:0809.0589.
- [32] K. Zhang, H. Li, P. Zhang, J. Yuan, J. Chen, W. Ren, Z. Wang, C. Song, D.-W. Wang, H. Wang, S. Zhu, G. S. Agarwal, and M. O. Scully, Synthesizing five-body interaction in a superconducting quantum circuit, Phys. Rev. Lett. 128, 190502 (2022), arXiv:2109.00964.
- [33] H.-Y. Huang, Y. Tong, D. Fang, and Y. Su, Learning many-body Hamiltonians with Heisenberg-limited scaling, Phys. Rev. Lett. 130, 200403 (2023), arXiv:2210.03030.
- [34] M. Ma, S. T. Flammia, J. Preskill, and Y. Tong, Learning k-body Hamiltonians via compressed sensing, arXiv:2410.18928 (2024).
- [35] H.-Y. Hu, M. Ma, W. Gong, Q. Ye, Y. Tong, S. T. Flammia, and S. F. Yelin, Ansatz-free Hamiltonian learning with Heisenberg-limited scaling, arXiv:2502.11900 (2025).
- [36] P. Baßler, M. Zipper, C. Cedzich, M. Heinrich, P. H. Huber, M. Johanning, and M. Kliesch, Synthesis of and compilation with time-optimal multi-qubit gates, Quantum 7, 984 (2023), arXiv:2206.06387.
- [37] P. Baßler, M. Heinrich, and M. Kliesch, Timeoptimal multi-qubit gates: Complexity, efficient heuristic and gate-time bounds, Quantum 8, 1279 (2024), arXiv:2307.11160.
- [38] G. Bhole, T. Tsunoda, P. J. Leek, and J. A. Jones, Rescaling interactions for quantum control, Phys. Rev. Applied 13, 034002 (2020), arXiv:1911.04806.
- [39] T. Tsunoda, G. Bhole, S. A. Jones, J. A. Jones, and P. J. Leek, Efficient Hamiltonian programming in qubit arrays with nearest-neighbor couplings, Phys. Rev. A 102, 032405 (2020), arXiv:2003.07815.
- [40] S. P. Boyd and L. Vandenberghe, Convex optimization (Cambridge University Press, Cambridge, UK; New York, 2004).
- [41] I. Bárány, A generalization of Carathéodory's theorem, Discrete Mathematics 40, 141 (1982).
- [42] D. A. Spielman and S.-H. Teng, Smoothed analysis of algorithms: Why the simplex algorithm usually takes polynomial time, Journal of the ACM 51, 385 (2004), arXiv:cs/0111050.
- [43] E. Bach and S. Huiberts, Optimal smoothed analysis of the simplex method, arXiv:2504.04197 (2025).
- [44] J. Farkas, Theorie der einfachen Ungleichungen, Journal für die Reine und Angewandte Mathematik 124, 1 (1902).
- [45] E. Stiemke, Über positive Lösungen homogener linearer Gleichungen, Mathematische Annalen 76, 340 (1915).
- [46] A. Agrawal, R. Verschueren, S. Diamond, and S. Boyd, A rewriting system for convex optimization problems, J. Control Decis. 5, 42 (2018), arXiv:1709.04494.
- [47] S. Diamond and S. Boyd, CVXPY: A Python-embedded modeling language for convex optimization, J. Mach. Learn. Res. 17, 1 (2016), arXiv:1603.00943.
- [48] MOSEK ApS, MOSEK Optimizer API for Python 9.3.14 (2022).
- [49] P. Baßler, Source code for "Efficient Hamiltonian engineering", https://github.com/paba92/EffHamEng (2024).
- [50] S. Hayakawa, T. Lyons, and H. Oberhauser, Estimating the probability that a given vector is in the convex hull of

- a random sample, Probability Theory and Related Fields **185**, 705 (2023), arXiv:2101.04250.
- [51] J. G. Wendel, A problem in geometric probability., MATHEMATICA SCANDINAVICA 11, 109–112 (1962).
- [52] U. Wagner and E. Welzl, A continuous analogue of the upper bound theorem, Discrete & Computational Geometry 26, 205 (2001).
- [53] F. Arute et al., Quantum supremacy using a programmable superconducting processor, Nature 574, 505 (2019), arXiv:1910.11333.
- [54] L. Schmid, D. F. Locher, M. Rispler, S. Blatt, J. Zeiher, M. Müller, and R. Wille, Computational capabilities and compiler development for neutral atom quantum processors—connecting tool developers and hardware experts, Quantum Sci. Technol. 9, 10.1088/2058-9565/ad33ac (2024), arXiv:2309.08656.
- [55] L. Henriet, L. Beguin, A. Signoles, T. Lahaye, A. Browaeys, G.-O. Reymond, and C. Jurczak, *Quantum computing with neutral atoms*, Quantum 4, 327 (2020), arXiv:2006.12326.
- [56] V. P. Canelles, M. G. Algaba, H. Heimonen, M. Papič, M. Ponce, J. Rönkkö, M. J. Thapa, I. de Vega, and A. Auer, *Benchmarking Digital-Analog Quantum Com*putation, arXiv:2307.07335 (2023).
- [57] U. Haeberlen and J. S. Waugh, Coherent averaging effects in magnetic resonance, Phys. Rev. 175, 453 (1968).
- [58] U. Haeberlen, High Resolution NMR in Solids (Academic Press, 1976).
- [59] W. Magnus, On the exponential solution of differential equations for a linear operator, Communications on Pure and Applied Mathematics 7, 649 (1954).
- [60] M. Bando, T. Ichikawa, Y. Kondo, and M. Nakahara, Concatenated composite pulses compensating simultaneous systematic errors, Journal of the Physical Society of Japan 82, 014004 (2013), arXiv:1209.4247.
- [61] S. Kukita, H. Kiya, and Y. Kondo, Short composite quantum gate robust against two common systematic errors, Journal of the Physical Society of Japan 91, 104001 (2022), arXiv:2112.12945.
- [62] B. T. Torosov and N. V. Vitanov, Composite pulses with errant phases, Phys. Rev. A 100, 023410 (2019), arXiv:1904.13168.
- [63] G. T. Genov, D. Schraft, T. Halfmann, and N. V. Vitanov, Correction of arbitrary field errors in population inversion of quantum systems by universal composite pulses, Phys. Rev. Lett. 113, 043001 (2014), arXiv:1403.1201.
- [64] G. T. Genov, M. Hain, N. V. Vitanov, and T. Halfmann, Universal composite pulses for efficient population inversion with an arbitrary excitation profile, Phys. Rev. A 101, 013827 (2020), arXiv:2002.08321.
- [65] H.-N. Wu, C. Zhang, J. Song, Y. Xia, and Z.-C. Shi, Composite pulses for optimal robust control in two-level systems, Phys. Rev. A 107, 023103 (2023).
- [66] C. Kabytayev, T. J. Green, K. Khodjasteh, M. J. Bier-cuk, L. Viola, and K. R. Brown, Robustness of composite pulses to time-dependent control noise, Phys. Rev. A 90, 012316 (2014), arXiv:1402.5174.
- [67] B. T. Torosov, S. S. Ivanov, and N. V. Vitanov, Narrowband and passband composite pulses for variable rotations, Phys. Rev. A 102, 013105 (2020), arXiv:2004.08456.
- [68] M. E. S. Morales, P. C. S. Costa, G. Pantaleoni, D. K. Burgarth, Y. R. Sanders, and D. W. Berry, Selection and

- improvement of product formulae for best performance of quantum simulation, arXiv:2210.15817 (2022).
- [69] H. F. Trotter, On the product of semi-groups of operators, Proceedings of the American Mathematical Society 10, 545 (1959).
- [70] M. Suzuki, General theory of fractal path integrals with applications to many-body theories and statistical physics, Journal of Mathematical Physics 32, 400 (1991).
- [71] A. M. Childs, Y. Su, M. C. Tran, N. Wiebe, and S. Zhu, Theory of Trotter error with commutator scaling, Phys. Rev. X 11, 011020 (2021), arXiv:1912.08854.
- [72] P. C. Moan and J. Niesen, Convergence of the Magnus series, Foundations of Computational Mathematics 8, 291 (2008), arXiv:0609198.
- [73] A. Brinkmann, Introduction to average Hamiltonian theory. I. Basics, Concepts in Magnetic Resonance Part A 45A, e21414 (2016).
- [74] K. Sharma and M. C. Tran, Hamiltonian simulation in the interaction picture using the Magnus expansion, arXiv:2404.02966 (2024).
- [75] H. K. Cummins, G. Llewellyn, and J. A. Jones, Tackling systematic errors in quantum logic gates with composite rotations, Phys. Rev. A 67, 042308 (2003), arXiv:quantph/0208092.
- [76] N. B. Karahanoğlu, H. Erdoğan, and Ş. İ. Birbil, A mixed integer linear programming formulation for the sparse recovery problem in compressed sensing, in 2013 IEEE International Conference on Acoustics, Speech and Signal Processing (2013) pp. 5870–5874.
- [77] C. Piltz, T. Sriarunothai, S. S. Ivanov, S. Wölk, and C. Wunderlich, Versatile microwave-driven trapped ion spin system for quantum information processing, Sci. Adv. 2, e1600093 (2016), arXiv:1509.01478.
- [78] A. Arnal, F. Casas, and C. Chiralt, A general formula for the Magnus expansion in terms of iterated integrals of right-nested commutators, Journal of Physics Communications 2, 035024 (2018), arXiv:1710.10851.

APPENDIX

Appendix A: Properties of solutions of (PauliLP)

In this section, we show the existence of solutions, provide lower and upper bounds on the relative evolution time, and discuss the tightness of these bounds. First, a direct consequence of proposition III.2 is that (PauliLP) is feasible or arbitrary Hamiltonians H_S and H_T satisfying $nz(\mathbf{A}) \subseteq nz(\mathbf{J})$.

Corollary A.1 (existence of solutions). Let

$$H_S = \sum_{\boldsymbol{a} \in \mathbb{F}_2^{2n} \setminus \{\boldsymbol{0}\}} J_{\boldsymbol{a}} P_{\boldsymbol{a}} \quad and \quad H_T = \sum_{\boldsymbol{a} \in \mathbb{F}_2^{2n} \setminus \{\boldsymbol{0}\}} A_{\boldsymbol{a}} P_{\boldsymbol{a}}, \tag{A1}$$

with $nz(A) \subseteq nz(J)$. Then the partial Walsh-Hadamard matrix $W^{(r \times 4^n)}$ with r = |nz(J)| leads to a feasible (PauliLP).

Proof. We know that all rows of the Walsh-Hadamard matrix are linearly independent. Furthermore, each row of the Walsh-Hadamard matrix sums to zero, thus x = 1 > 0 is a solution to $W^{(r \times 4^n)}x = 0$. By proposition III.2 we know that (PauliLP) always has a feasible solution even if we consider an arbitrary subset of rows.

To bound the optimal solutions $\mathbf{1}^T \lambda^*$ of (PauliLP) we define the dual LP

maximize
$$\boldsymbol{M}^T \boldsymbol{y}$$

subject to $(W^{(r \times 4^n)})^T \boldsymbol{y} \leq \mathbf{1}, \, \boldsymbol{y} \in \mathbb{R}^r$. (A2)

As in the previously considered case of two-body Ising interactions [37], we have the following bounds on the value of (PauliLP):

Theorem A.2 (bounds on solutions). The optimal objective function value of (PauliLP) with a partial Walsh-Hadamard matrix $W^{(r \times 4^n)}$ is bounded by

$$\|\boldsymbol{M}\|_{\ell_{\infty}} \leq \mathbf{1}^{T} \boldsymbol{\lambda}^{*} \leq \|\boldsymbol{M}\|_{\ell_{1}}. \tag{A3}$$

Proof. The lower bound can be verified by the fact that $W^{(r \times 4^n)}$ in (PauliLP) only has entries ± 1 and that λ^* is non-negative. Thus, it holds that $\|M\|_{\ell_{\infty}} = \|W^{(r \times 4^n)}\lambda^*\|_{\ell_{\infty}} \leq \mathbf{1}^T\lambda^*$.

To show the upper bound, we first define the set of feasible solutions for the dual LP (A2)

$$\mathcal{F} := \left\{ \boldsymbol{y} \in \mathbb{R}^r \mid (W^{(r \times 4^n)})^T \boldsymbol{y} \le \mathbf{1} \right\}. \tag{A4}$$

Next, consider the partial Walsh-Hadamard matrix $W^{((4^n-1)\times 4^n)}$ without the first row, corresponding to the identity Pauli term $P_{\boldsymbol{a}} = I^{\otimes n}$ with $\boldsymbol{a} = \boldsymbol{0}$. We show that

$$S := \left\{ \boldsymbol{y} \in \mathbb{R}^{4^{n} - 1} \mid (W^{((4^{n} - 1) \times 4^{n})})^{T} \boldsymbol{y} \le 1 \right\}$$
(A5)

is a simplex. A simplex is formed by affine independent vectors. Vectors of the form $(1, v_i)^T$ are linearly dependent if and only if the vectors v_i are affine dependent. From linear dependence it follows that there is a vector $t \neq 0$ such that $\sum_i t_i (1, \boldsymbol{v}_i)^T = \mathbf{0}$. Thus $\sum_i t_i = 0$ and $\sum_i v_i = \mathbf{0}$, and the vectors \boldsymbol{v}_i are affine dependent. For any n, the Walsh-Hadamard matrix $W = (\mathbf{1}, (W^{((4^n-1)\times 4^n)})^T)$ has linearly independent rows and columns. Therefore, $W^{((4^n-1)\times 4^n)}$ has affine independent columns, and \mathcal{S} forms a simplex. With $\mathcal{H} = \{\boldsymbol{y} \in \mathbb{R}^{4^n-1} | \|\boldsymbol{y}\|_{\ell_\infty} \leq 1\}$ we denote the 4^n-1 dimensional hypercube. Note that the rows of $W^{(r\times 4^n)}$ are rows of the $4^n\times 4^n$ dimensional Walsh-Hadamard matrix. We define the embedding $g: \mathbb{R}^r \to \mathbb{R}^{(4^n)-1}$ by appending zeros, such that $(W^{(r\times 4^n)})^T \boldsymbol{y} = (W^{((4^n-1)\times 4^n)})^T g(\boldsymbol{y})$. Therefore the objective value of the dual LP (A2) can be upper bounded as follows

$$\max_{\boldsymbol{y} \in \mathcal{F}} \langle \boldsymbol{M}, \boldsymbol{y} \rangle = \max_{g(\boldsymbol{y}) \in \mathcal{S}} \langle g(\boldsymbol{M}), g(\boldsymbol{y}) \rangle
\leq \max_{\boldsymbol{x} \in \mathcal{S}} \langle g(\boldsymbol{M}), \boldsymbol{x} \rangle
\leq \max_{\boldsymbol{x} \in \mathcal{H}} \langle g(\boldsymbol{M}), \boldsymbol{x} \rangle = \|\boldsymbol{M}\|_{\ell_1}.$$
(A6)

The upper bound for $\mathbf{1}^T \boldsymbol{\lambda}^*$ follows by strong duality.

Next, we show a (not complete) set of instances of (PauliLP), yielding solutions λ^* which satisfy the upper bound of theorem A.2. Such M constitute the worst cases.

Proposition A.3. If $M \in \{-\boldsymbol{w}_i \mid \boldsymbol{w}_i \text{ is the } i\text{-th column of } W^{((4^n-1)\times 4^n)}\}$, then $\mathbf{1}^T \boldsymbol{\lambda}^* = \|\boldsymbol{M}\|_{\ell_1}$.

Proof. Let $y = -w_i$ be a negative column of $W^{((4^n-1)\times 4^n)}$. Then, by orthogonality of the rows/columns of the Walsh-Hadamard matrix, we obtain

$$\left((W^{(4^n - 1) \times 4^n)})^T (-\boldsymbol{w}_i) \right)_j = \begin{cases} -(4^n - 1), & i = j \\ 1, & \text{otherwise}. \end{cases}$$
(A7)

Therefore, $\mathbf{y} = -\mathbf{w}_i$ is a feasible solution $(W^{((4^n-1)\times 4^n)})^T\mathbf{y} \leq \mathbf{1}$ to the dual LP (A2). The dual objective function value is $\mathbf{M}^T\mathbf{y} = \|\mathbf{w}_i\|_{\ell_1} = 4^n - 1$. Next, we show a feasible solution of (PauliLP). For a $\mathbf{M} = -\mathbf{w}_i$ define

$$\lambda_j = \begin{cases} 0, & i = j \\ 1, & \text{otherwise} . \end{cases}$$
 (A8)

Clearly, this satisfies $W^{((4^n-1)\times 4^n)}\boldsymbol{\lambda} = -\boldsymbol{w}_i$. Furthermore, the primal objective function value $\mathbf{1}^T\boldsymbol{\lambda} = 4^n - 1$ is the same as for the dual objective function value, which shows optimality. It is easy to see that $\|\boldsymbol{M}\|_{\ell_1} = 4^n - 1$.

Appendix B: Comments on the efficient relaxation for the Pauli conjugation

As mentioned in the main text, Wendel's theorem is applicable to spherical symmetric distributions. This would imply that sampling a certain column from $W^{(r \times 4^n)}$ has the same probability as sampling the same column with a flipped sign. Recall that for a partial Walsh-Hadamard matrix $W_{ab}^{(r \times 4^n)} = (-1)^{\langle a,b \rangle}$, with $\langle a,b \rangle = a_x \cdot b_z + a_z \cdot b_x$. It holds that

$$W_{ab}^{(r \times 4^n)} = -W_{a\bar{b}}^{(r \times 4^n)} \quad \forall a, b \in \mathbb{F}_2^{2n}, \tag{B1}$$

for $|a| = 1 \mod 2$ and with the binary complement \bar{b} is given element-wise given by $\bar{x} := 1 - x$ for any $x \in \{0, 1\}$. If the decomposition of H_S has only terms $J_a P_a$ with odd |a|, then we can apply Wendel's theorem directly. In this case, we have a success probability of 1/2 to find a feasible $W^{(r \times 2r)}$ (with r interactions) if we sample 2r many $b \in \mathbb{F}_2^{2n}$ uniformly random. However, an example of such a Hamiltonian with two-body interactions is

$$H = \sum_{i=1}^{n} \left(J_i^X X_i + J_i^Y Y_i \right) + \sum_{i \neq j}^{n} \left(J_{ij}^{XZ} X_i Z_j + J_{ij}^{YZ} Y_i Z_j \right), \tag{B2}$$

and with commuting interactions is

$$H = \sum_{i=1}^{n} J_i^X X_i + \sum_{ijk}^{n} J_{ijk}^{XXX} X_i X_j X_k ,$$
 (B3)

with arbitrary coupling constants. Unfortunately, for a general Hamiltonian, we cannot use Wendel's theorem to construct a relaxation for (PauliLP).

Recently, lower bounds on $p_{s,x}$ have been proposed for arbitrary distributions [50]. However, their results rely on the halfspace depth (or Tukey depth), which is hard to compute. It is a measure of how extreme a point is with respect to a distribution of random points.

Definition B.1 (halfspace depth). Let x be an arbitrary r-dimensional random vector. Then, the halfspace depth at the origin is defined as

$$\alpha_{\boldsymbol{x}} := \inf_{\|\boldsymbol{c}\|=1} \mathbb{P}(\boldsymbol{c}^T \boldsymbol{x} \le \boldsymbol{0}). \tag{B4}$$

The halfspace depth α_x is the minimum (fraction) number of points in a halfspace with the origin on the boundary.

Theorem B.2 ([50, Theorem 14]). Let x be an arbitrary r-dimensional random vector. Then, for each positive integer $s \geq 3r/\alpha_x$, we have

$$p_{s,x} > 1 - \frac{1}{2^r}$$
 (B5)

Let \boldsymbol{w} be a r-dimensional random vector drawn uniformly from $\operatorname{col}(W^{(r \times 4^n)})$. From corollary A.1, we find the trivial lower bound $1/4^n \leq \alpha_{\boldsymbol{w}}$, since at least one point is in an arbitrary halfspace with the origin on its boundary. Finding a constant lower bound $1/\beta \leq \alpha_{\boldsymbol{w}}$ would imply that for $s \geq 3r\beta$ we find a feasible $W^{(r \times s)}$ with high probability. One needs to show that at least $4^{O(n)}$ points are contained in an arbitrary halfspace with the origin on its boundary.

Appendix C: Proofs for the general robust conjugation method

We provide the proofs for section IV B. Some proofs provide more technical details which aims for an easy implementation into a programming language. For the sake of easy readability we repeat the definitions of the main text.

Definition IV.1. Let $\mathcal{G} \subset \text{Herm}(\mathbb{C}^2)$ be a set of single-qubit pulse generators. A single-qubit pulse layer is given by a local generator h_i chosen from \mathcal{G} for each qubit $i \in [n]$, the (single-qubit) rotation directions $\mathbf{s} \in \mathbb{F}_2^n$ and the finite pulse time $t_p > 0$. The Hamiltonian generating the single-qubit pulse layer on n qubits is given by

$$H(t_p, \boldsymbol{s}, \boldsymbol{h}) := \frac{1}{t_p} \sum_{i=1}^n (-1)^{s_i} h_i, \qquad (41)$$

with $\mathbf{h} := (h_1, \dots, h_n)$. The single-qubit pulse layer Hamiltonian is completely specified by the tuple $c := (t_p, \mathbf{s}, \mathbf{h})$, and we write $H_c := H(t_p, \mathbf{s}, \mathbf{h})$. This generates the evolution operator for one single-qubit pulse layer

$$\mathbf{S}_c(t) \coloneqq \mathrm{e}^{-\mathrm{i}tH_c}, \quad and \quad \mathbf{S}_c \coloneqq \mathbf{S}_c(t_p).$$
 (42)

More generally, we consider a sequence of n_L single-qubit pulse layers and introduce the layer index $\ell \in [n_L]$. The evolution for the ℓ -th single-qubit pulse layer is specified by the tuple $c^{(\ell)} := (t_p^{(\ell)}, \mathbf{s}^{(\ell)}, \mathbf{h}^{(\ell)})$, and we define the tuple $\mathbf{c} := (c^{(1)}, \dots, c^{(n_L)})$. Moreover, we define the single-qubit pulse block and the partial single-qubit pulse block as

$$S_{c} := \prod_{\ell=1}^{n_{L}} S_{c^{(\ell)}}, \qquad (43)$$

and

$$\boldsymbol{S}_{\boldsymbol{c}^{\geq D}} := \begin{cases} \overrightarrow{\prod}_{\ell=D}^{n_L} \boldsymbol{S}_{c^{(\ell)}}, & 1 \leq D \leq n_L \\ \mathbb{1}, & otherwise, \end{cases}$$
(44)

respectively. Similarly, we define the pulse time for the single-qubit pulse block $T_p := \sum_{\ell=1}^{n_L} t_p^{(\ell)}$ and for the partial single-qubit pulse block $T_p^{\leq D} := \sum_{\ell=1}^{D} t_p^{(\ell)}$.

We consider the time evolution

$$U(t\lambda_{c}) = \left(\prod_{\ell=1}^{\underline{n_{L}}} e^{-it_{p}^{(\ell)}(H_{S} - H_{c(\ell)})} \right) e^{-it\lambda_{c}H_{S}} \left(\prod_{\ell=1}^{\underline{n_{L}}} e^{-it_{p}^{(\ell)}(H_{S} + H_{c(\ell)})} \right), \tag{C1}$$

with the finite duration of the ℓ -th pulse layer $0 < t_p^{(\ell)}$.

Lemma IV.2. The approximation of $U(t\lambda_c)$ in first order Magnus expansion is given by $e^{-iH_{av,c}(t)}$ with

$$H_{\text{av.}c}(t) = t\lambda_c S_c^{\dagger} H_S S_c + H_{\text{err.}c}, \tag{46}$$

where

$$H_{\operatorname{err}, \mathbf{c}} := 2 \sum_{\ell=1}^{n_L} \mathbf{S}_{\mathbf{c}^{\geq(\ell+1)}}^{\dagger} \int_0^{t_p^{(\ell)}} \mathbf{S}_{c^{(\ell)}}^{\dagger}(t) H_S \mathbf{S}_{c^{(\ell)}}(t) dt \, \mathbf{S}_{\mathbf{c}^{\geq(\ell+1)}}.$$

$$(47)$$

The average Hamiltonian $H_{\mathrm{av},\mathbf{c}}(t)$ has the same interaction graph as H_S . Moreover, the error for truncating the Magnus expansion after the first order can be bounded in spectral norm by

$$||U(t\lambda_c) - e^{-iH_{av,c}(t)}|| \le O((2T_p + t\lambda_c)^2 ||H_S||^2).$$
 (48)

Proof. We consider the time evolution during the ℓ -th layer of single-qubit pulses in the interaction frame with respect to the single-qubit pulse Hamiltonian $H_{c(\ell)}$ [57, 73]

$$e^{-it_p^{(\ell)}(H_S \pm H_{c^{(\ell)}})} = e^{\mp it_p^{(\ell)} H_{c^{(\ell)}}} \mathcal{U}_{\pm}^{(\ell)}(t_p^{(\ell)}) = S_{c^{(\ell)}}^{\pm 1} \mathcal{U}_{\pm}^{(\ell)}(t_p^{(\ell)}),$$
(C2)

with the interaction frame propagator $\mathcal{U}_{\pm}^{(\ell)}(t_p^{(\ell)})$. The interaction frame propagator has to fulfill

$$\frac{d\mathcal{U}_{\pm}^{(\ell)}(t)}{dt} = -\mathrm{i}\left(\boldsymbol{S}_{c^{(\ell)}}^{\mp 1}(t)H_{S}\boldsymbol{S}_{c^{(\ell)}}^{\pm 1}(t)\right)\mathcal{U}_{\pm}^{(\ell)}(t). \tag{C3}$$

Inserting eq. (C2) into eq. (C1) yields

$$U(t\lambda_{\mathbf{c}}) = \left(\prod_{\ell=1}^{\underline{n_L}} \mathbf{S}_{c^{(\ell)}}^{-1} \mathcal{U}_{-}^{(\ell)}(t_p^{(\ell)}) \right) e^{-it\lambda_{\mathbf{c}} H_S} \left(\prod_{\ell=1}^{\underline{n_L}} \mathbf{S}_{c^{(\ell)}} \mathcal{U}_{+}^{(\ell)}(t_p^{(\ell)}) \right). \tag{C4}$$

We define $\tilde{\mathcal{U}}_{-}^{(\ell)}(t)$ as

$$\frac{d\tilde{\mathcal{U}}_{-}^{(\ell)}(t)}{dt} := \boldsymbol{S}_{\boldsymbol{c}^{\geq \ell}}^{-1} \frac{d\mathcal{U}(\ell)_{-}(t)}{dt} \boldsymbol{S}_{\boldsymbol{c}^{\geq \ell}} = -\mathrm{i} \left(\boldsymbol{S}_{\boldsymbol{c}^{\geq \ell}}^{-1} \boldsymbol{S}_{c^{(\ell)}}(t) H_{S} \boldsymbol{S}_{\boldsymbol{c}^{(\ell)}}^{-1}(t) \boldsymbol{S}_{\boldsymbol{c}^{\geq \ell}} \right) \tilde{\mathcal{U}}_{-}^{(\ell)}(t), \tag{C5}$$

and $\tilde{\mathcal{U}}_{+}^{(\ell)}(t)$ as

$$\frac{d\tilde{\mathcal{U}}_{+}^{(\ell)}(t)}{dt} := \boldsymbol{S}_{\boldsymbol{c}^{\geq (\ell+1)}}^{-1} \frac{d\mathcal{U}(\ell)_{+}(t)}{dt} \boldsymbol{S}_{\boldsymbol{c}^{\geq (\ell+1)}} = -\mathrm{i} \left(\boldsymbol{S}_{\boldsymbol{c}^{\geq (\ell+1)}}^{-1} \boldsymbol{S}_{\boldsymbol{c}^{(\ell)}}^{-1}(t) H_{S} \boldsymbol{S}_{\boldsymbol{c}^{(\ell)}}(t) \boldsymbol{S}_{\boldsymbol{c}^{\geq (\ell+1)}} \right) \tilde{\mathcal{U}}_{+}^{(\ell)}(t); \tag{C6}$$

where $\tilde{\mathcal{U}}_{-}^{(\ell)}(t)$ and $\tilde{\mathcal{U}}_{+}^{(\ell)}(t)$ are defined such that we can commute the exact evolution of the single-qubit pulse layers to the free evolution under H_S . It directly follows that

$$U(t\lambda_{\mathbf{c}}) = \left(\prod_{\ell=1}^{\underline{n_L}} \tilde{\mathcal{U}}_{-}^{(\ell)}(t)\right) e^{-it\lambda_{\mathbf{c}} \mathbf{S}_{\mathbf{c}}^{-1} H_S \mathbf{S}_{\mathbf{c}}} \left(\prod_{\ell=1}^{\underline{n_L}} \tilde{\mathcal{U}}_{+}^{(\ell)}(t)\right). \tag{C7}$$

The Hamiltonian governing the evolution of $U(t\lambda_c)$ is defined piecewise as

$$H_{\boldsymbol{c}}(\tilde{t}) \coloneqq \begin{cases} \boldsymbol{S}_{\boldsymbol{c}^{\geq (\ell+1)}}^{-1} \boldsymbol{S}_{\boldsymbol{c}^{(\ell)}}^{-1}(\tilde{t}) H_{S} \boldsymbol{S}_{\boldsymbol{c}^{(\ell)}}(\tilde{t}) \boldsymbol{S}_{\boldsymbol{c}^{\geq (\ell+1)}} , & T_{p}^{\leq (\ell-1)} \leq \tilde{t} < T_{p}^{\leq \ell} \\ \boldsymbol{S}_{\boldsymbol{c}}^{-1} H_{S} \boldsymbol{S}_{\boldsymbol{c}} , & T_{p} \leq \tilde{t} < T_{p} + t \lambda_{\boldsymbol{c}} \\ \boldsymbol{S}_{\boldsymbol{c}^{\geq \ell}}^{-1} \boldsymbol{S}_{\boldsymbol{c}^{(\ell)}}(\tilde{t}) H_{S} \boldsymbol{S}_{\boldsymbol{c}^{(\ell)}}^{-1}(\tilde{t}) \boldsymbol{S}_{\boldsymbol{c}^{\geq \ell}} , & T_{p} + T_{p}^{\leq (\ell-1)} + t \lambda_{\boldsymbol{c}} \leq \tilde{t} < T_{p} + T_{p}^{\leq \ell} + t \lambda_{\boldsymbol{c}} . \end{cases}$$
(C8)

The effective Hamiltonian is approximated by the first-order term in the Magnus expansion up to time $T = 2T_p + t\lambda_c$, yielding the time independent average Hamiltonian

$$H_{\text{av},c}(t) = \int_{0}^{T} H_{c}(\tilde{t}) d\tilde{t}$$

$$= t \lambda_{c} S_{c}^{-1} H_{S} S_{c} + \sum_{\ell=1}^{n_{L}} S_{c^{\geq(\ell+1)}}^{-1} \int_{0}^{t_{p}^{(\ell)}} S_{c^{(\ell)}}^{-1}(t) H_{S} S_{c^{(\ell)}}(t) dt S_{c^{\geq(\ell+1)}} + S_{c^{\geq\ell}}^{-1} \int_{0}^{t_{p}^{(\ell)}} S_{c^{(\ell)}}(t) H_{S} S_{c^{(\ell)}}^{-1}(t) dt S_{c^{\geq\ell}}$$

$$= t \lambda_{c} S_{c}^{-1} H_{S} S_{c} + 2 \sum_{\ell=1}^{n_{L}} S_{c^{\geq(\ell+1)}}^{-1} \int_{0}^{t_{p}^{(\ell)}} S_{c^{(\ell)}}^{-1}(t) H_{S} S_{c^{(\ell)}}(t) dt S_{c^{\geq(\ell+1)}}.$$
(C9)

We denote the term corresponding to the finite pulse time error by

$$H_{\text{err},c} := 2 \sum_{\ell=1}^{n_L} S_{c^{\geq (\ell+1)}}^{-1} \int_0^{t_p^{(\ell)}} S_{c^{(\ell)}}^{-1}(t) H_S S_{c^{(\ell)}}(t) dt S_{c^{\geq (\ell+1)}}.$$
 (C10)

Then, the average Hamiltonian is

$$H_{\text{av},c}(t) = t\lambda_c S_c^{-1} H_S S_c + H_{\text{err},c}.$$
(C11)

Note, that conjugation of the system Hamiltonian H_S with single-qubit operations as in $\mathbf{S}_{c}^{-1}H_{S}\mathbf{S}_{c}$ and $H_{\text{err},c}$ always preserves the locality and thus the interaction graph of H_S .

Finally, we prove the error bounds on the truncation of the Magnus expansion after the first order. The k-th order term of the Magnus expansion can be written as

$$H_{\text{av}}^{(k)} = \sum_{\sigma \in S_k} (-1)^{d_b} \frac{d_a! d_b!}{k!} \int_0^T d\tau_1 \int_0^{\tau_1} d\tau_2 \cdots \int_0^{\tau_{k-1}} d\tau_k H_c(\tau_{\sigma(1)}) H_c(\tau_{\sigma(2)}) \dots H_c(\tau_{\sigma(k)}), \qquad (C12)$$

where $T = 2T_p + t\lambda_c$, S_k denotes the group of permutations σ of the set [k] the number of ascents d_a and descents d_b are defined as

$$d_a := |\{i \in [k-1] \mid \sigma(i) < \sigma(i+1)\}| \quad \text{and} \quad d_b := |\{i \in [k-1] \mid \sigma(i) > \sigma(i+1)\}|,$$
 (C13)

and it holds that $d_a + d_b = k$ [78]. Finally, we argue that

$$||H_{\text{av}}^{(k)}|| \le O\left((2T_p + t\lambda_c)^k ||\max_{\tau \in [0, 2T_p + t\lambda_c]} H_c(\tau)||^k\right) = O((2T_p + t\lambda_c)^k ||H_S||^k),$$
(C14)

where the equality follows from the definition of $H_c(\tau) = U^{-1}H_SU$ for some unitaries U and the invariance of the spectral norm under unitary transformation. The error bound in spectral norm follows from the Duhamel principle in Ref. [74, App. A]

$$||U(t\lambda_{c}) - e^{-iH_{av,c}(t)}|| \le \sum_{k=2}^{\infty} ||H_{av}^{(k)}|| = O((2T_{p} + t\lambda_{c})^{2} ||H_{S}||^{2}),$$
 (C15)

assuming that $||H_{\rm av}^{(2)}|| > \sum_{k=3}^{\infty} ||H_{\rm av}^{(k)}||$, i.e.} the Magnus expansion converges.

Lemma IV.3. Let $W(J)^{(r \times s)}$, $E(J)^{(r \times s)} \in \mathbb{R}^{r \times s}$ be the matrices representing the ideal conjugation and the finite pulse time error in the Pauli basis respectively. The entries are given by

$$W(\boldsymbol{J})_{\boldsymbol{a}\boldsymbol{c}}^{(r\times s)} := \frac{1}{2^n} \operatorname{Tr} \left(P_{\boldsymbol{a}} \left(\boldsymbol{S}_{\boldsymbol{c}}^{\dagger} H_S \boldsymbol{S}_{\boldsymbol{c}} \right) \right) , \tag{49}$$

and

$$E(\boldsymbol{J})_{\boldsymbol{ac}}^{(r \times s)} \coloneqq \frac{1}{2^n} \operatorname{Tr} \left(P_{\boldsymbol{a}} H_{\operatorname{err}, \boldsymbol{c}} \right) ,$$
 (50)

and can be calculated in polynomial time in the number of qubits for a local system Hamiltonian H_S .

Proof. Recall, that the system Hamiltonian has the form

$$H_S = \sum_{\boldsymbol{a} \in \mathbb{F}_2^{2n} \setminus \{\mathbf{0}\}} J_{\boldsymbol{a}} P_{\boldsymbol{a}} \,. \tag{C16}$$

Let $H_{c(\ell)} = \frac{\theta^{(\ell)}}{t_p^{(\ell)}} \sum_{i=1}^n (-1)^{s_i^{(\ell)}} h_i^{(\ell)}$ be an arbitrary layer of single-qubit rotations, with the rotation angle $\theta^{(\ell)}$, the pulse duration $t_p^{(\ell)}$ the generators $h_i^{(\ell)} \coloneqq p_{x,i}^{(\ell)} X + p_{y,i}^{(\ell)} Y + p_{z,i}^{(\ell)} Z$ and the rotation direction $s_i^{(\ell)} \in \mathbb{F}_2$. For the sake of a clear notation we omit the layer index (ℓ) for now. The single-qubit pulse on the i-th qubit can be written as

$$S_{c_i}(t) := e^{-it\frac{\theta}{t_p}h_i} = \cos(t\frac{\theta}{t_p})I - i(-1)^{s_i}\sin(t\frac{\theta}{t_p})h_i.$$
 (C17)

Then, $S_c(t) = e^{-itH_c} = \bigotimes_{i=1}^n S_{c_i}(t)$. The conjugation with a single-qubit pulse layer changes the interaction term as

$$S_c^{-1}(t)J_a P_a S_c(t) = J_a \bigotimes_{i=1}^n S_{c_i}^{-1}(t) P_{a_i} S_{c_i}(t).$$
(C18)

The effect of such a conjugation on the i-th qubit is given by

$$S_{c_i}^{-1}(t)P_{\boldsymbol{a}_i}S_{c_i}(t) = \cos^2(\tilde{\theta})P_{\boldsymbol{a}_i} + \sin^2(\tilde{\theta})h_iP_{\boldsymbol{a}_i}h_i + \mathrm{i}[h_i, P_{\boldsymbol{a}_i}](-1)^{s_i}\sin(\tilde{\theta})\cos(\tilde{\theta}), \tag{C19}$$

with $\tilde{\theta} := t \frac{\theta}{t_p}$. Equation (C19) can be further decomposed into Pauli terms $S_{c_i}^{-1}(t) P_{\boldsymbol{a}_i} S_{c_i}(t) = g_{x,i}(\tilde{\theta}) X + g_{y,i}(\tilde{\theta}) Y + g_{z,i}(\tilde{\theta}) Z$, with

$$\begin{split} g_{x,i}(\tilde{\theta}) &\coloneqq \begin{cases} \cos^2(\tilde{\theta}) + (p_{x,i}^2 - p_{y,i}^2 - p_{z,i}^2) \sin^2(\tilde{\theta}) \,, & \text{if } P_{\boldsymbol{a}_i} = X \\ 2p_{x,i}p_{y,i}\sin^2(\tilde{\theta}) + 2p_{z,i}(-1)^{s_i}\sin(\tilde{\theta})\cos(\tilde{\theta}) \,, & \text{if } P_{\boldsymbol{a}_i} = Y \\ 2p_{x,i}p_{z,i}\sin^2(\tilde{\theta}) - 2p_{y,i}(-1)^{s_i}\sin(\tilde{\theta})\cos(\tilde{\theta}) \,, & \text{if } P_{\boldsymbol{a}_i} = Z \,, \end{cases} \\ g_{y,i}(\tilde{\theta}) &\coloneqq \begin{cases} 2p_{x,i}p_{y,i}\sin^2(\tilde{\theta}) + 2p_{z,i}(-1)^{s_i}\sin(\tilde{\theta})\cos(\tilde{\theta}) \,, & \text{if } P_{\boldsymbol{a}_i} = X \\ \cos^2(\tilde{\theta}) + (p_{y,i}^2 - p_{x,i}^2 - p_{z,i}^2)\sin^2(\tilde{\theta}) \,, & \text{if } P_{\boldsymbol{a}_i} = Y \\ 2p_{y,i}p_{z,i}\sin^2(\tilde{\theta}) - 2p_{x,i}(-1)^{s_i}\sin(\tilde{\theta})\cos(\tilde{\theta}) \,, & \text{if } P_{\boldsymbol{a}_i} = Z \,, \end{cases} \\ g_{z,i}(\tilde{\theta}) &\coloneqq \begin{cases} 2p_{x,i}p_{z,i}\sin^2(\tilde{\theta}) - 2p_{y,i}(-1)^{s_i}\sin(\tilde{\theta})\cos(\tilde{\theta}) \,, & \text{if } P_{\boldsymbol{a}_i} = X \\ 2p_{y,i}p_{z,i}\sin^2(\tilde{\theta}) + 2p_{x,i}(-1)^{s_i}\sin(\tilde{\theta})\cos(\tilde{\theta}) \,, & \text{if } P_{\boldsymbol{a}_i} = X \\ \cos^2(\tilde{\theta}) + (p_{z,i}^2 - p_{x,i}^2 - p_{y,i}^2)\sin^2(\tilde{\theta}) \,, & \text{if } P_{\boldsymbol{a}_i} = Z \,, \end{cases} \end{split}$$

and if $P_{a_i} = I$, then $S_{c_i}^{-1}(t)P_{a_i}S_{c_i}(t) = I$. Assume, that the interaction J_aP_a is k-local, i.e. the interaction acts on the qubits $i \in \text{supp}(a)$ and |supp(a)| = k. Applying $A \otimes (B + C) = A \otimes B + A \otimes C$ the conjugation in eq. (C18) yields

$$\bigotimes_{i=1}^{n} S_{c_{i}}^{-1}(t) P_{\boldsymbol{a}_{i}} S_{c_{i}}(t) = \sum_{\substack{\tilde{\boldsymbol{a}} \in \mathbb{F}_{2}^{n} \\ \text{supp}(\tilde{\boldsymbol{a}}) = \text{supp}(\boldsymbol{a})}} \left(\prod_{i \in \tilde{\boldsymbol{a}}} g_{\tilde{\boldsymbol{a}}_{i}, i}(\tilde{\boldsymbol{\theta}}) \right) P_{\tilde{\boldsymbol{a}}}, \tag{C21}$$

where we identify $g_{(1,0),i} = g_{x,i}$, $g_{(1,1),i} = g_{y,i}$ and $g_{(0,1),i} = g_{z,i}$. This sum has at most 3^k terms, which is constant for a system Hamiltonian H_S with a fixed interaction graph.

With that we are ready to compute $E(J)_{ac}^{(r \times s)}$ by calculating the Pauli coefficients of

$$H_{\text{err},c} = 2 \sum_{\ell=1}^{S} \mathbf{S}_{c^{\geq(\ell+1)}}^{-1} \int_{0}^{t_{p}^{(\ell)}} \mathbf{S}_{c^{(\ell)}}^{-1}(t) H_{S} \mathbf{S}_{c^{(\ell)}}(t) dt \, \mathbf{S}_{c^{\geq(\ell+1)}}.$$
 (C22)

We start with the integral

$$\int_{0}^{t_{p}^{(\ell)}} \mathbf{S}_{c^{(\ell)}}^{-1}(t) H_{S} \mathbf{S}_{c^{(\ell)}}(t) dt = \sum_{\boldsymbol{a} \in \mathbb{F}_{2}^{2n} \setminus \{\mathbf{0}\}} J_{\boldsymbol{a}} \int_{0}^{t_{p}^{(\ell)}} \bigotimes_{i=1}^{n} S_{c_{i}^{(\ell)}}^{-1}(t) P_{\boldsymbol{a}_{i}} S_{c_{i}^{(\ell)}}(t) dt
= \sum_{\boldsymbol{a} \in \mathbb{F}_{2}^{2n} \setminus \{\mathbf{0}\}} \sum_{\substack{\tilde{\boldsymbol{a}} \in \mathbb{F}_{2}^{n} \\ \text{supp}(\tilde{\boldsymbol{a}}) = \text{supp}(\boldsymbol{a})}} J_{\boldsymbol{a}} \frac{t_{p}^{(\ell)}}{\theta^{(\ell)}} \int_{0}^{\theta^{(\ell)}} \left(\prod_{i \in \tilde{\boldsymbol{a}}} g_{\tilde{\boldsymbol{a}}_{i}, i}(\tilde{\boldsymbol{\theta}}) \right) d\tilde{\boldsymbol{\theta}} P_{\tilde{\boldsymbol{a}}}$$

$$=: \sum_{\boldsymbol{a} \in \mathbb{F}_{2}^{2n} \setminus \{\mathbf{0}\}} E_{\boldsymbol{a}}^{(\ell)} P_{\boldsymbol{a}},$$
(C23)

where $E_{\boldsymbol{a}}^{(\ell)}$ can be efficiently calculated by integrating trigonometric polynoms and summing all contributions from the terms with the same support $\sup(\tilde{\boldsymbol{a}}) = \sup(\boldsymbol{a})$. Next, the conjugation $S_{\boldsymbol{c}^{\geq (\ell+1)}}^{-1}(\cdot) S_{\boldsymbol{c}^{\geq (\ell+1)}}$ in eq. (C22) corresponds to applying eq. (C21) for each $\tilde{\ell} = 1, \ldots, \ell+1$ to $E_{\boldsymbol{a}}^{(\ell)} P_{\boldsymbol{a}}$ with $t = t_p^{(\tilde{\ell})}$ or $\tilde{\theta} = \theta^{(\tilde{\ell})}$. Then, we obtain

$$H_{\text{err},c} = \sum_{\boldsymbol{a} \in \mathbb{F}_2^{2n} \setminus \{\boldsymbol{0}\}} E(\boldsymbol{J})_{\boldsymbol{a}\boldsymbol{c}}^{(r \times s)} P_{\boldsymbol{a}}. \tag{C24}$$

The entries of $W(\boldsymbol{J})^{(r\times s)}$ can be calculated similarly by applying eq. (C21) for each $\ell=1,\ldots,n_L$ to $J_{\boldsymbol{a}}P_{\boldsymbol{a}}$ with $t=t_p^{(\ell)}$ or $\tilde{\theta}=\theta^{(\ell)}$. Together, we obtain

$$S_{\mathbf{c}}^{-1}H_{S}S_{\mathbf{c}} = \sum_{\mathbf{a} \in \mathbb{F}_{2}^{2n} \setminus \{\mathbf{0}\}} W(\mathbf{J})_{\mathbf{a}\mathbf{c}}^{(r \times s)} P_{\mathbf{a}}.$$
 (C25)

Appendix D: Proofs for the robust Pauli conjugation method

Lemma IV.9. Consider all labels $\mathbf{a} \in \mathbb{F}_2^{2n}$ for the non-zero interactions $J_{\mathbf{a}} \neq 0$ in the system Hamiltonian. Then, the approximation of $U(t\lambda_{\mathbf{c}})$ for the Pauli conjugation in first order Magnus expansion is given by $e^{-iH_{av,\mathbf{c}}(t)}$ with

$$H_{\text{av},c}(t) = t\lambda_c S_c^{\dagger} H_S S_c + H_{\text{err},c}, \qquad (54)$$

where

$$H_{\text{err},c} = \sum_{\boldsymbol{a} \in \mathbb{F}_2^{2n} \setminus \{\boldsymbol{0}\}} \left(J_{\boldsymbol{a}} E_{\boldsymbol{a},c}^{(r \times s)} P_{\boldsymbol{a}} + R_{\boldsymbol{a},c} \right). \tag{55}$$

We call the first term in eq. (55) the interaction term, with

$$E_{\boldsymbol{a},\boldsymbol{c}}^{(r\times s)} := \frac{4t_p}{\pi} \int_0^{\frac{\pi}{2}} \left(\prod_{i \in \text{supp}(\boldsymbol{a})} (\cos^2(\theta) + (-1)^{\langle \boldsymbol{a}_i, \boldsymbol{b}_i \rangle} \sin^2(\theta)) \right) d\theta,$$
(56)

which we collect as entries of the matrix $E^{(r \times s)} \in \mathbb{R}^{r \times s}$. We call the second term $R_{\boldsymbol{a},\boldsymbol{c}}$ the rest term, and it is proportional to $(-1)^{\boldsymbol{e_a} \cdot \boldsymbol{s}}$, with $\boldsymbol{s} \in \mathbb{F}_2^n$ representing the chosen rotation direction of the π pulses and $\boldsymbol{e_a} \in \mathbb{F}_2^n$ encodes the sign flips due to the finite pulse time error such that $\boldsymbol{e_{a,i}} = 0$ for all $i \notin \operatorname{supp}(\boldsymbol{a})$.

Proof. From lemma IV.2 with $n_L = 1$ and $H_c = H_{c^{(1)}}$ we get the Hamiltonian corresponding to the finite pulse time effect

$$H_{\text{err},\boldsymbol{c}} := 2 \int_0^{t_p} e^{itH_{\boldsymbol{c}}} H_S e^{-itH_{\boldsymbol{c}}} dt.$$
 (D1)

Recall, that the system Hamiltonian has the form

$$H_S = \sum_{\boldsymbol{a} \in \mathbb{F}_2^{2n} \setminus \{\boldsymbol{0}\}} J_{\boldsymbol{a}} P_{\boldsymbol{a}} \,. \tag{D2}$$

Before we compute $H_{\mathrm{err},c}$ we investigate the conjugation $\mathrm{e}^{\mathrm{i}tH_c}H_S\mathrm{e}^{-\mathrm{i}tH_c}$ for a single-qubit. A π pulse on the i-th qubit can be written as

$$S_{c_i}(t) := e^{-it\frac{\pi}{2t_p}(-1)^{s_i}P_{b_i}} = \cos\left(\frac{\pi}{2}\frac{t}{t_p}\right)I - i(-1)^{s_i}P_{b_i}\sin\left(\frac{\pi}{2}\frac{t}{t_p}\right) = \cos(\theta)I - i(-1)^{s_i}P_{b_i}\sin(\theta), \quad (D3)$$

with the Pauli generator P_b from eq. (11) and $\theta(t) := \frac{\pi}{2} \frac{t}{t_p}$. Then the effect of the conjugation on the *i*-th qubit is given by

$$S_{c_i}^{-1}(\theta)P_{\boldsymbol{a}_i}S_{c_i}(\theta) = \underbrace{\left(\cos^2(\theta) + (-1)^{\langle \boldsymbol{a}_i, \boldsymbol{b}_i \rangle} \sin^2(\theta)\right)}_{=:\alpha_{\boldsymbol{a}_i, \boldsymbol{b}_i}(\theta)} P_{\boldsymbol{a}_i} + (-1)^{s_i} \underbrace{\cos(\theta) \sin(\theta)}_{\beta(\theta)} i[P_{\boldsymbol{b}_i}, P_{\boldsymbol{a}_i}]$$

$$= \alpha_{\boldsymbol{a}_i, \boldsymbol{b}_i}(\theta)P_{\boldsymbol{a}_i} + (-1)^{s_i}\beta(\theta)i[P_{\boldsymbol{b}_i}, P_{\boldsymbol{a}_i}],$$
(D4)

with the binary symplectic form $\langle \cdot, \cdot \rangle$ from eq. (2) and the commutator $[\cdot, \cdot]$. Let

$$F(e) := \begin{cases} P_{\boldsymbol{a}} \alpha_{\boldsymbol{a}_i, \boldsymbol{b}_i}(\theta), & e = 0 \\ i[P_{\boldsymbol{b}_i}, P_{\boldsymbol{a}_i}] \beta(\theta), & e = 1. \end{cases}$$
 (D5)

(D6)

Inserting H_S in eq. (D1) and applying $A \otimes (B+C) = A \otimes B + A \otimes C$ yields

$$H_{\text{err},c} = \frac{4t_p}{\pi} \sum_{\boldsymbol{a} \in \mathbb{F}_2^{2^n} \setminus \{\boldsymbol{0}\}} J_{\boldsymbol{a}} \int_0^{\frac{\pi}{2}} \left(\bigotimes_{i \in \text{supp}(\boldsymbol{a})} (P_{\boldsymbol{a}_i} \alpha_{\boldsymbol{a}_i, \boldsymbol{b}_i}(\boldsymbol{\theta}) + i[P_{\boldsymbol{b}_i}, P_{\boldsymbol{a}_i}] \beta(\boldsymbol{\theta})(-1)^{s_i}) \right) d\boldsymbol{\theta}$$

$$= \frac{4t_p}{\pi} \sum_{\boldsymbol{a} \in \mathbb{F}_2^{2^n} \setminus \{\boldsymbol{0}\}} \left(J_{\boldsymbol{a}} \int_0^{\frac{\pi}{2}} \prod_{i \in \text{supp}(\boldsymbol{a})} \alpha_{\boldsymbol{a}_i, \boldsymbol{b}_i}(\boldsymbol{\theta}) d\boldsymbol{\theta} P_{\boldsymbol{a}} + \sum_{\substack{\boldsymbol{e} \in \mathbb{F}_2^n \setminus \{\boldsymbol{0}\}\\e_i = 0 \ \forall i \notin \text{supp}(\boldsymbol{a})}} \left(\prod_{i \in \text{supp}(\boldsymbol{a})} (-1)^{e_i + s_i} \right) \left(\bigotimes_{i \in \text{supp}(\boldsymbol{a})} F(e_i) \right) \right)$$

$$= \sum_{\boldsymbol{a} \in \mathbb{F}_2^{2^n} \setminus \{\boldsymbol{0}\}} J_{\boldsymbol{a}} E_{\boldsymbol{a}, \boldsymbol{c}}^{(r \times s)} P_{\boldsymbol{a}} + \sum_{\substack{\boldsymbol{e} \in \mathbb{F}_2^n \setminus \{\boldsymbol{0}\}\\e_i = 0 \ \forall i \notin \text{supp}(\boldsymbol{a})}} (-1)^{\boldsymbol{e} \cdot \boldsymbol{s}} \bigotimes_{i \in \text{supp}(\boldsymbol{a})} F(e_i).$$

Moreover, we define $E_{\boldsymbol{a},\boldsymbol{c}}^{(r\times s)} := \frac{4t_p}{\pi} \int_0^{\frac{\pi}{2}} \left(\prod_{i \in \text{supp}(\boldsymbol{a})} \alpha_{\boldsymbol{a}_i,\boldsymbol{b}_i}(\theta) \right) d\theta$. To conclude, we have the average Hamiltonian

$$H_{\text{av},c}(t) = t\lambda_c S_c^{\dagger} H_S S_c + H_{\text{err},c},$$
 (D7)

from lemma IV.2, and we calculated the finite pulse time error term

$$H_{\text{err},c} = \sum_{\boldsymbol{a} \in \mathbb{F}_2^{2n} \setminus \{\boldsymbol{0}\}} \left(J_{\boldsymbol{a}} E_{\boldsymbol{a},\boldsymbol{c}}^{(r \times s)} P_{\boldsymbol{a}} + R_{\boldsymbol{a},\boldsymbol{c}} \right) , \tag{D8}$$

with

$$E_{\boldsymbol{a},\boldsymbol{c}}^{(r\times s)} := \frac{4t_p}{\pi} \int_0^{\frac{\pi}{2}} \left(\prod_{i \in \text{supp}(\boldsymbol{a})} (\cos^2(\theta) + (-1)^{\langle \boldsymbol{a}_i, \boldsymbol{b}_i \rangle} \sin^2(\theta)) \right) d\theta$$
 (D9)

and

$$R_{\boldsymbol{a},\boldsymbol{c}} := \sum_{\substack{\boldsymbol{e} \in \mathbb{F}_2^n \setminus \{\boldsymbol{0}\}\\ e_i = 0 \ \forall i \notin \operatorname{supp}(\boldsymbol{a})}} (-1)^{\boldsymbol{e} \cdot \boldsymbol{s}} \bigotimes_{i \in \operatorname{supp}(\boldsymbol{a})} F(e_i),$$
(D10)

which proofs the lemma.

Proposition IV.11. Let the rotation directions $s \in \mathbb{F}_2^n$ of the π pulses such that $\sum_s (-1)^{e_{\boldsymbol{a}} \cdot s} = 0$ for all $e_{\boldsymbol{a}} \in \mathbb{F}_2^n$ with $e_{\boldsymbol{a},i} = 0$ for all $i \notin \operatorname{supp}(\boldsymbol{a})$ for any \boldsymbol{a} with $J_{\boldsymbol{a}} \neq 0$, as in lemma IV.9. Then, the rotation angle errors in the first order Taylor approximation cancels.

Proof. We model the rotation angle error of a perfect π pulse $e^{-i(-1)^{s_i}\frac{\pi}{2}P_{b_i}}$ with the rotation direction $(-1)^{s_i}$ and $s_i \in \mathbb{F}_2$ by

$$\tilde{S}_{c_i} = e^{-i(-1)^{s_i} \frac{\pi + \varepsilon_i}{2} P_{b_i}} = -\frac{\varepsilon_i}{2} \operatorname{Id} -i(-1)^{s_i} P_{b_i} + O(\varepsilon_i^2),$$
(D11)

where we used the first-order Taylor expansion of sine and cosine. Conjugating a Pauli operator with an imperfect Pauli pulse results in

$$\tilde{S}_{c_i}^{\dagger} P_{\boldsymbol{a}_i} \tilde{S}_{c_i} = P_{\boldsymbol{b}_i} P_{\boldsymbol{a}_i} P_{\boldsymbol{b}_i} + \mathrm{i}(-1)^{s_i} \frac{\varepsilon_i}{2} [P_{\boldsymbol{a}_i}, P_{\boldsymbol{b}_i}] + \mathrm{O}(\varepsilon_i^2). \tag{D12}$$

We use the identity $U^{\dagger}e^{-itH}U = e^{-itU^{\dagger}HU}$ to compute the effective Hamiltonian of a system Hamiltonian H_S conjugated with a layer of imperfect Pauli pulses $\tilde{\boldsymbol{S}}_{\boldsymbol{c}} = \bigotimes_{i=1}^n \tilde{S}_{c_i}$,

$$\tilde{S}_{c}^{\dagger}H_{S}\tilde{S}_{c} = \sum_{\boldsymbol{a}\in\mathbb{F}_{2}^{2n}\setminus\{\boldsymbol{0}\}} J_{\boldsymbol{a}}\bigotimes_{i=1}^{n} \left(\tilde{S}_{c_{i}}^{\dagger}P_{\boldsymbol{a}_{i}}\tilde{S}_{c_{i}}\right) \\
= \sum_{\boldsymbol{a}\in\mathbb{F}_{2}^{2n}\setminus\{\boldsymbol{0}\}} J_{\boldsymbol{a}}\bigotimes_{i=1}^{n} \left(P_{\boldsymbol{b}_{i}}P_{\boldsymbol{a}_{i}}P_{\boldsymbol{b}_{i}} + i(-1)^{s_{i}}\frac{\varepsilon_{i}}{2}[P_{\boldsymbol{a}_{i}},P_{\boldsymbol{b}_{i}}] + O(\varepsilon_{i}^{2})\right) \\
= \sum_{\boldsymbol{a}\in\mathbb{F}_{2}^{2n}\setminus\{\boldsymbol{0}\}} \left(J_{\boldsymbol{a}}P_{\boldsymbol{b}}P_{\boldsymbol{a}}P_{\boldsymbol{b}} + \sum_{\substack{\boldsymbol{e}\in\mathbb{F}_{2}^{n}\\e_{i}=0\,\forall i\notin\operatorname{supp}(\boldsymbol{a})}} \left(\prod_{i\in\operatorname{supp}(\boldsymbol{a})} (-1)^{e_{i}+s_{i}}\varepsilon_{i}^{e_{i}}\right) \left(\bigotimes_{i\in\operatorname{supp}(\boldsymbol{a})} F(e_{i}) + O(\varepsilon_{i}^{2})\right)\right), \tag{D13}$$

where we used $A \otimes (B + C) = A \otimes B + A \otimes C$ and

$$F(e) := \begin{cases} P_{\mathbf{b}_i} P_{\mathbf{a}_i} P_{\mathbf{b}_i}, & e = 0\\ i \frac{1}{2} [P_{\mathbf{a}_i}, P_{\mathbf{b}_i}], & e = 1. \end{cases}$$
(D14)

The second term in the sum is the first-order angle error contribution, and has the same sign structure $(-1)^{e_i+s_i}$ as the rest term $R_{\boldsymbol{a},\boldsymbol{c}}$ in eq. (D6). Therefore, choosing the signs $\boldsymbol{s} \in \mathbb{F}_2^n$, such that the rest term $R_{\boldsymbol{a},\boldsymbol{c}}$ cancels, simultaneously cancels the first order angle error contribution in eq. (D13).

The proof of the following result is similar as the proof in [37, Lemma 8].

Proposition IV.12. Let $\kappa = 2^{\lceil \log_2(n+1) \rceil} \leq 2n$ and let $W^{(\kappa \times \kappa)}$ be the $\kappa \times \kappa$ dimensional Walsh-Hadamard matrix. Choose n distinct columns from $W^{(\kappa \times \kappa)}$ without the first column and define the resulting partial Walsh-Hadamard matrix as $W^{(\kappa \times n)}$. Let $(-1)^{s_{(j)}}$ be the j-th row of $W^{(\kappa \times n)}$. Then, for $\mathbf{a} \in \mathbb{F}_2^{2n}$ and $\mathbf{e}_{\mathbf{a}} \in \mathbb{F}_2^n$ with $|\operatorname{supp}(\mathbf{a})| = 2$ and $\mathbf{e}_{\mathbf{a},i} = 0$ for all $i \notin \operatorname{supp}(\mathbf{a})$ we obtain $\sum_{j=1}^{\kappa} (-1)^{\mathbf{e}_{\mathbf{a}} \cdot \mathbf{s}_{(j)}} = 0$.

Proof. From the choice of $(-1)^{s_{(j)}}$ it directly follows that $\sum_{j=1}^{\kappa} (-1)^{e \cdot s_{(j)}} = 0$ for all $e \in \mathbb{F}_2^n$ with |e| = 1, since the sum over all rows of a Walsh-Hadamard matrix especially $W^{(\kappa \times n)}$ is zero. We now have to show that $\sum_{j=1}^{\kappa} (-1)^{e \cdot s_{(j)}} = 0$ for all $e \in \mathbb{F}_2^n$ with |e| = 2. For any $e \in \mathbb{F}_2^n$ with |e| = 2 we can write $(-1)^{e \cdot s} = (-1)^{s_i} (-1)^{s_k} = \left(((-1)^s)((-1)^s)^T\right)_{ik}$ with $i, k \in [n]$ and $i \neq k$. Then, we obtain

$$\sum_{j=1}^{\kappa} (-1)^{\boldsymbol{e} \cdot \boldsymbol{s}_{(j)}} = \sum_{j=1}^{\kappa} \left(((-1)^{\boldsymbol{s}_{(j)}}) ((-1)^{\boldsymbol{s}_{(j)}})^T \right)_{ik}, \tag{D15}$$

with $i, k \in [n]$ and $i \neq k$. The orthogonality property of the Walsh-Hadamard matrix yields

$$\sum_{j=1}^{\kappa} ((-1)^{s_{(j)}}) ((-1)^{s_{(j)}})^{T} = (W^{(\kappa \times n)})^{T} W^{(\kappa \times n)} = \kappa I,$$
(D16)

where the non-diagonal entries $i \neq k$ correspond to the sum eq. (D15) and are zero.